Drug Research Program
Division of Pharmaceutical Chemistry and Technology
Faculty of Pharmacy
University of Helsinki
Finland

Imitation of biologically relevant oxidation reactions by titanium dioxide photocatalysis:

Advances in understanding the mimicking of drug metabolism and the oxidation of phosphopeptides

Miina Ruokolainen

ACADEMIC DISSERTATION

To be presented, with permission of the Faculty of Pharmacy of the University of Helsinki, for public examination in Auditorium 1041, Viikki Biocenter 2 on October 27th 2017, at 12 noon.

Helsinki 2017

ISBN 978-951-51-3713-5 (paperback)
ISBN 978-951-51-3714-2 (PDF)
ISSN 2342-3161 (print)
ISSN 2342-317X (online)
http://ethesis.helsinki.fi/

Published in
Dissertationes Scholae Doctoralis Ad Sanitatem Investigandam Universitatis Helsinkiensis

Unigrafia
Helsinki 2017

Supervisors

Professor Risto Kostiainen
Drug Research Program
Division of Pharmaceutical Chemistry and Technology
Faculty of Pharmacy
University of Helsinki
Finland

Professor Tapio Kotiaho
Drug Research Program
Division of Pharmaceutical Chemistry and Technology
Faculty of Pharmacy
and
Department of Chemistry
Faculty of Science
University of Helsinki
Finland

Docent Tiina Sikanen
Drug Research Program
Division of Pharmaceutical Chemistry and Technology
Faculty of Pharmacy
University of Helsinki
Finland

Reviewers

Professor Rainer Bischoff
Department of Analytical Biochemistry
Faculty of Science and Engineering
University of Groningen
The Netherlands

Docent Ari Tolonen
Admescope Ltd.
Finland

Opponent

Associate Professor Christian Janfelt
Department of Pharmacy, Section of Analytical Biosciences
Faculty of Health and Medical Sciences
University of Copenhagen
Denmark

Abstract

Redox reactions play an important role in human physiology and pathophysiology. For example, oxidative stress and free radical-mediated oxidation of proteins and lipids are implicated in several diseases such as Alzheimer's and Parkinson's disease. Oxidation reactions belong also to the most important phase I metabolism pathways of drugs, which can give rise to pharmacologically active or toxic metabolites. The established methods for *in vitro* drug metabolism studies, e.g. methods using hepatocytes, human liver microsomes (HLMs), and recombinant enzymes, are relatively time-consuming and expensive. Thus, the potential of several nonenzymatic oxidation methods, such as those based on metalloporphyrins, electrochemistry (EC), and Fenton reaction, have been explored for metabolism studies. However, new methods need to be developed to enable rapid production of drug metabolite standards and since none of the above nonenzymatic methods allow comprehensive prediction of phase I drug metabolism.

The titanium dioxide (TiO_2) photocatalysis method was developed and applied to evaluate the effect of phosphorylation of tyrosine on the oxidation of (phospho)peptides with the same sequence but different phosphorylation states. The results obtained using ultra-high-performance liquid chromatography – mass spectrometry (UHPLC-MS) show that nonphosphorylated tyrosine was the amino acid most susceptible to hydroxyl radical-initiated oxidation, but oxidation of tyrosine was in most cases inhibited by its phosphorylation.

The feasibility of TiO_2 photocatalysis for imitation of *in vitro* phase I HLM metabolism of small drug molecules was studied using UHPLC-MS and compared with the electrochemically assisted Fenton reaction (EC-Fenton) and EC. TiO_2 photocatalysis, EC-Fenton, and EC imitated 44%, 31%, and 11%, respectively, of the *in vitro* phase I HLM metabolites of four model compounds. As TiO_2 photocatalysis proved most feasible for the imitation of *in vitro* phase I HLM metabolism, its feasibility for imitation of *in vitro* phase I HLM metabolism of five anabolic steroids was also examined. TiO_2 photocatalysis was able to imitate over half of the hydroxylation and dehydrogenation metabolites, but its imitation of the metabolites resulting from combinations of these reactions was considerably poorer.

To enable even more rapid experiments to study biologically relevant oxidation reactions, TiO_2-photocatalysis was simply integrated with desorption electrospray ionization (DESI)-MS by using the same TiO_2-coated glass wafer for photocatalytic reactions and DESI-MS analysis. This new method enabled high-throughput investigation of photocatalytic oxidation reactions, as demonstrated using 12 model compounds, and imitation of several drug metabolism reactions of three model compounds studied in more detail.

In conclusion, TiO_2 photocatalysis proved a feasible method for oxidation of compounds with different polarities. TiO_2 photocatalysis cannot predict drug metabolism comprehensively, but offers a potential method for rapid, simple, and inexpensive study of oxidation reactions of biomolecules and imitation of several drug metabolism reactions. Preparative scale synthesis of oxidation products by TiO_2 photocatalysis is likely an alternative application of the method, but this remains to be demonstrated.

Acknowledgements

This work was carried out at the Division of Pharmaceutical Chemistry and Technology at the Faculty of Pharmacy, University of Helsinki, Finland during 2010-2017. A part of the study was carried out at the Analytical Biochemistry, Department of Pharmacy, University of Groningen, The Netherlands, in May 2013. Funding by the Finnish Cultural Foundation, the Finnish Concordia Fund, the CHEMSEM Graduate School, and the University of Helsinki is gratefully acknowledged.

I am deeply grateful to my supervisors, Professor Tapio Kotiaho, Professor Risto Kostiainen, and Docent Tiina Sikanen, for guidance and support as well as constructive criticism and space to grow as an independent researcher. With admirable enthusiasm and dedication to science, they were always available for discussions and advice and full of ideas. Special thanks to Tapio for being such an encouraging and helpful boss over the years.

I am indebted to all of my collaborators and coauthors. First and foremost, I thank Elisa Ollikainen and Minna Valkonen for performing the experimental part of their Master's thesis in my research project. It was delightful to supervise them as they performed all tasks with enthusiasm and diligence. I am grateful to Dr. Hjalmar Permentier for welcoming me into his laboratory and giving me the opportunity to learn electrochemical techniques, and Turan Gul for helping me with practicalities in the lab. The atmosphere in the group was inspiring, and the month that I spent in Groningen gave me abundant new insights and developed me as a scientist. I acknowledge Dr. Ville Miikkulainen, who fabricated the TiO_2 coating, and Professor Mikko Ritala for providing their expertise in atomic layer deposition and for efficient collaboration. The official reviewers, Professor Rainer Bischoff and Docent Ari Tolonen, are thanked for insightful comments and a rapid review. In addition, warm thanks go to Dr. Anu Vaikkinen, Dr. Markus Haapala, Dr. Petri Kylli, and Marja Hagström for assistance with practical issues in the lab.

The head of our division, Professor Jari Yli-Kauhaluoma, is acknowledged for being a great boss, always willing to help. I am also thankful to all past and present colleagues at the Division of Pharmaceutical Chemistry for the great atmosphere, everyone being eager to help, and for making work enjoyable in the lab and office, and especially during coffee breaks. *Kampai* to the conference team of Tini, Titti, Marja, and Petri for the funniest times in science life! I'm also grateful for having the opportunity to participate in teaching, which I enjoyed immensely. Warm thanks to the teaching staff, especially to Dr. Katariina Vuorensola.

I'm grateful to my dear friends for taking my mind off work and worries. Finally, my warmest gratitude is owed to my family. I thank my parents for always supporting me. Enormous thanks to Mikko for his never-ending support, understanding, and love, and to our daughter Halla for being the sunshine of our lives.

Espoo August 2017

Miina Ruokolainen

Contents

List of original publications

This thesis is based on the following publications:

I Ruokolainen, M., Ollikainen, E., Sikanen, T., Kotiaho, T., Kostiainen, R., *Oxidation of Tyrosine-Phosphopeptides by Titanium Dioxide Photocatalysis*, J. Am. Chem. Soc. 138 (2016) 7452–7455.

II Ruokolainen, M., Gul, T., Permentier, H., Sikanen, T., Kostiainen, R., Kotiaho, T., *Comparison of TiO_2 photocatalysis, electrochemically assisted Fenton reaction and direct electrochemistry for simulation of phase I metabolism reactions of drugs*, Eur. J. Pharm. Sci. 83 (2016) 36–44.

III Ruokolainen, M., Valkonen, M., Sikanen, T., Kotiaho, T., Kostiainen, R., *Imitation of phase I oxidative metabolism of anabolic steroids by titanium dioxide photocatalysis*, Eur. J. Pharm. Sci. 65 (2014) 45–55.

IV Ruokolainen, M., Miikkulainen, V., Ritala, M., Sikanen, T., Kotiaho, T., Kostiainen, R., *TiO_2 photocatalysis–DESI-MS rotating array platform for high-throughput investigation of oxidation reactions*, accepted for publication in Anal. Chem.

These publications are referred to in the text by their Roman numerals. They have been reprinted here with the permission of their copyright holders.

Author's contributions

I. The experimental work was carried out by the author with some contribution from Elisa Ollikainen. The manuscript was written by the author with contributions from the coauthors.

II. The experimental work was carried out by the author. The manuscript was written by the author with contributions from the coauthors.

III. The experimental work was carried out by Minna Valkonen and supervised by the author. The manuscript was written by the author with contributions from the coauthors.

IV. The experimental work was carried out by the author, excluding fabrication and characterization of the TiO_2 films and synthesis of D-amphetamine. The manuscript was written by the author with contributions from the coauthors.

Abbreviations

ACN	Acetonitrile
ALD	Atomic layer deposition
CYP450	Cytochrome P450
D	Aspartic acid
DESI	Desorption electrospray ionization
DOPA	3,4-dihydroxyphenylalanine residue
e^-	Electron
E	Glutamic acid
EC	Electrochemistry
EC-acidic	Electrochemical experiments in acidic conditions
EC-basic	Electrochemical experiments in basic conditions
EC-Fenton	Electrochemically assisted Fenton reaction
EDTA	Ethylenediaminetetraacetic acid disodium salt dehydrate
ESI	Electrospray ionization
h^+	Hole
HLMs	Human liver microsomes
HRMS	High-resolution mass spectrometry/high-resolution mass spectrometer
H_2O_2	Hydrogen peroxide
$HO_2^{\bullet}$	Hydroperoxide
HOCl	Hypochlorous acid
I	Isoleucine
IR0	TRDIYETDYYRK
IR1A	TRDIpYETDYYRK
IR1B	TRDIYETDpYYRK
IR1C	TRDIYETDYpYRK
IR3	TRDIpYETDpYpYRK
K	Lysine
LC	Liquid chromatography
MS	Mass spectrometry/mass spectrometer
MS/MS	Tandem mass spectrometry
m/z	Mass-to-charge ratio
µPESI	Micropillar electrospray ionization
NADPH	β-nicotinamide adenine dinucleotide 2′-phosphate reduced tetrasodium salt
NO	Nitric oxide
$^{\bullet}NO_2$	Nitrogen dioxide
$^1O_2$	Singlet oxygen
$O_2^{\bullet-}$	Superoxide anion
O_3	Ozone
$^{\bullet}OH$	Hydroxyl radical
$ONOO^-$	Peroxynitrite
p	Phosphorylated
R	Arginine

$RO^{\bullet}$	Alkoxyl radical
$ROO^{\bullet}$	Peroxyl radical
ROS	Reactive oxygen species
Q	Quadrupole
T	Threonine
TiO_2	Titanium dioxide
TiOH	Titanol
TOF	Time-of-flight
t_R	Retention time
TTIP	Titanium(IV) isopropoxide
UHPLC	Ultra-high-performance liquid chromatography
UV	Ultraviolet radiation
Y	Tyrosine

1 Introduction

Redox reactions play a major role in several physiological and pathophysiological processes in the human body. For example, oxidative stress and free radical-mediated oxidation of biomolecules are implicated in aging and a wide spectrum of diseases, including neurodegenerative diseases, such as Parkinson's and Alzheimer's disease and amyotrophic lateral sclerosis, stroke, central nervous system injuries, cardiovascular diseases, such as atherosclerosis, chronic inflammation, diabetes, obesity, and several cancers.[1-5] Oxidation reactions are also among the most important phase I metabolism pathways of xenobiotics such as drugs[6] and carcinogens[7]. Considering the fundamental role of oxidation reactions in human health, it is essential to develop methods for studying and imitating these reactions. The work described in this thesis was aimed at developing and applying titanium dioxide (TiO_2) photocatalytic methods for oxidation of (phospho)peptides, imitation of phase I oxidative metabolism, and rapid screening of oxidation products.

1.1 Oxidative stress and protein oxidation by reactive oxygen species

Reactive oxygen species (ROS) are produced at low levels in normal metabolic processes of mammalian cells such as cellular respiration and various enzyme functions.[8] ROS are involved as signaling molecules in the regulation of cell proliferation, apoptosis, and gene expression.[4, 9] Phagocytes generate ROS as an essential defence mechanism in microbial infections. Intensive physical activity, pollutants or toxins, such as cigarette smoke, alcohol, and pesticides, ionizing and ultraviolet radiations (UV), and ozone also trigger generation of ROS. Transition metal-catalyzed "Fenton-like" reactions are an important source of ROS in cells.

Oxidative stress results from excessive ROS production relative to the cell's capacity for ROS detoxification.[9] ROS include hydroxyl radical ($^{\bullet}OH$), superoxide anion ($O_2^{\bullet-}$), singlet oxygen ($^1O_2$), hydrogen peroxide (H_2O_2), hydroperoxide ($HO_2^{\bullet}$), alkoxyl ($RO^{\bullet}$) and peroxyl ($ROO^{\bullet}$) radical, ozone (O_3), and hypochlorous acid (HOCl).[10] Also reactive nitrogen species, such as nitric oxide (NO), nitrogen dioxide ($^{\bullet}NO_2$), and peroxynitrite ($ONOO^-$), are involved in oxidative stress. Reactions of ROS often produce other ROS. For example, superoxide is the primary ROS created in mitochondrial respiration. It is not very reactive towards biological macromolecules. Instead, it reacts with superoxide dismutase to produce hydrogen peroxide, which can further react with metal ions or metal complexes to form hydroxyl radicals. Hydroxyl radical is the most aggressive oxidant species and responsible for most of the oxidative damage of biomolecules.[9]

Hydroxyl radicals can react with all classes of biomolecules such as lipids, proteins, and nucleic acids.[9] Proteins are the most abundant organic components of most biological systems[8] and are major initial targets of hydroxyl radicals in the cells.[11] Oxidative damage to proteins is mainly irreversible.[2, 8] While some oxidations of cysteine and methionine can be reduced enzymatically, mostly the fate of oxidatively damaged proteins is proteolysis.[8] Extensive oxidative modifications, cross-linking, and aggregation can render proteins

resistant to proteolysis.[12] Proteolysis is also diminished in aging and diseases associated with the accumulation of oxidized proteins such as atherosclerosis, cataract, rheumatoid arthritis, Alzheimer's disease, Parkinson's disease, and amyotrophic lateral sclerosis.

Identification of oxidative modifications *in vivo* is important to find biomarkers possibly facilitating diagnosis of diseases. Redox proteomics aims at identification of oxidatively or nitrosatively modified proteins.[2] For example, protein carbonylation and tyrosine nitrosylation are markers of oxidative stress.

1.2 Drug metabolism

Drug metabolism in general facilitates the elimination of drugs from the body. Drug-metabolizing enzymes are present in all tissues, but the main drug-metabolizing organ is the liver.[13] Drug metabolism is often divided into phases I and II. Phase I involves functionalization reactions, such as oxidation, reduction, or hydrolysis, where a functional group is attached to or exposed in a drug molecule. Phase II involves conjugation reactions that facilitate detoxification or excretion of the drug from the body. Phase I metabolism plays a key role in the bioactivation of drugs, as phase I reactions may give rise to pharmacologically active, toxic, or reactive metabolites.[14, 15] The most important phase I metabolic pathways are oxidation reactions catalyzed by cytochrome P450 (CYP450) isoenzymes.[16]

Detailed understanding of the metabolism of a drug candidate is essential at all stages of drug discovery and development in view of drug safety and pharmacokinetics.[15, 17] Drug metabolism is studied early in the drug discovery phase, as the metabolic stability, major metabolites, main metabolism routes, and metabolizing enzymes and their kinetics need to be determined before selection of lead and candidate molecules.[17] Drug metabolism is preliminary studied *in vitro* using e.g. liver slices, hepatocytes, complementary DNA-expressed recombinant enzymes, or subcellular fractions such as human liver microsomes (HLMs) or S9 fraction. Whole cell systems, i.e. liver slices and hepatocytes, give the most complete view of hepatic metabolism, as all metabolizing enzymes and cofactors are present.[18] Thus, the *in vitro/in vivo* correlation in whole cell systems is superior to that of subcellular fractions, and both enzyme induction and inhibition can be studied.[13, 17] In addition, hepatocytes and liver slices allow metabolite identification as well as evaluation of kinetics and metabolizing enzymes. Subcellular fractions are prepared by differential centrifugation of the liver homogenate.[19] The microsomes are vesicles derived from the hepatocyte smooth endoplasmatic reticulum and contain the CYP450 enzymes and phase II uridine 5'-diphospho-glucuronosyltransferase enzymes, whereas the cytosolic fraction contains most phase II enzymes. The S9 fraction contains both the cytosolic and the microsomal fractions, thus including both phase I and phase II enzymes. Subcellular fractions can be used to identify metabolites and study enzyme kinetics, metabolizing enzymes, and enzyme inhibition, but require addition of cofactors.[17] Recombinant enzymes allow the study of metabolizing enzymes and enzyme inhibition. Even though the well-established *in vitro* methods yield abundant metabolic information, pharmacokinetic

profile and toxicity need to be determined in a rodent and non-rodent animal species before clinical studies.[20]

As drug metabolism is nowadays studied in the early stages of the drug discovery process, the number of compounds to be tested is large, producing the need for faster, cheaper, and more convenient methods than the traditional *in vitro* methods, which are relatively time-consuming and expensive. In addition, drug metabolites must be produced, e.g. for analytical standards and toxicity testing, and can be sometimes difficult to synthesize.

1.3 Oxidation methods for *in vitro* protein research and imitation of drug metabolism

Oxidation of proteins *in vitro* allows the study of oxidative modifications and oxidation mechanisms in a less complex environment without biological interferences. Oxidation of proteins has also been exploited in proteomics, e.g. to facilitate sample preparation and purification, to alter chromatographic retention properties, to specifically cleave proteins, and to enable protein footprinting.[21] In protein footprinting, protein structure and conformational changes are studied by monitoring solvent accessibility.[22] The parts of the protein that are exposed to the solvent/environment are modified by reactive species. The locations of the oxidized amino acids can be analyzed using liquid chromatography – mass spectrometry (LC-MS) and used to determine the tertiary or quaternary structure of the protein or the interface region of two interacting proteins.[23]

As the most important phase I metabolic reactions are oxidation reactions catalyzed by CYP450 isoenzymes, various nonenzymatic oxidation methods, such as metalloporphyrins,[24] electrochemical reactions,[25, 26] Fenton reaction,[27-29] and TiO_2 photocatalysis[30, 31], have been studied from the perspective of providing faster, more convenient, and affordable alternatives to metabolite screening and production in the early preclinical phase. Although the exact reaction mechanism may differ from the enzymatic route, many CYP450 reactions can be simulated by these methods (Table 1).

Several methods have been used for oxidation of proteins and drugs, and the following sections focus on hydroxyl radical-based oxidation methods, direct electrochemistry (EC), and metalloporphyrins, as these are the most relevant considering the scope of this thesis.

Table 1. *Summary of the imitation of the most common phase I drug metabolism reactions by Fenton reaction, direct electrochemistry, metalloporphyrins, and TiO_2 photocatalysis.*

Reaction	Fenton	EC	Metallo-porphyrins	TiO_2
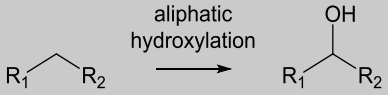 aliphatic hydroxylation	x	Indirect EC, Direct EC: only allylic and benzylic hydroxylation	x	x
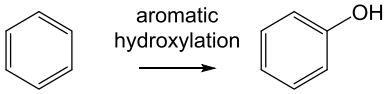 aromatic hydroxylation	x	Indirect EC, Direct EC: only hydroxylation of aromatic rings with activating substituents	x	x
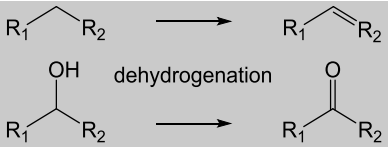 dehydrogenation	x	x	x	x
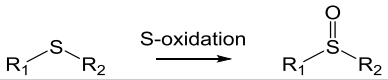 S-oxidation	x	x	x	
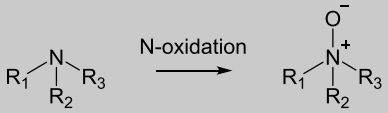 N-oxidation	x	x	x	
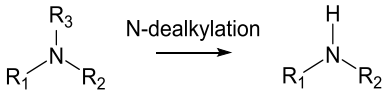 N-dealkylation	x	x	x	x
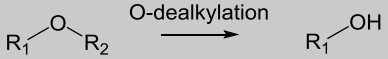 O-dealkylation	x	Poorly imitated, *ipso*-substitution of aromatic rings more likely	x	x

Fenton reactions are from refs. [26-29, 32-35]
Electrochemical reactions are from refs. [25, 26, 36-42]
Metalloporphyrin reactions are from refs. [26, 43]
TiO_2 photocatalytic reactions are from refs. [30, 31, 44-46]

1.3.1 Hydroxyl radical-based methods

Hydroxyl radicals can be generated from water or hydrogen peroxide by various chemical, photochemical, electrochemical, or electrophysical methods.[21, 22, 47] Even though hydroxyl radicals can be regarded as the main oxidative species, also other ROS, such as superoxide, hydroperoxide, and hydrogen peroxide, are often formed.[22]

In the Fenton reaction,[48] hydrogen peroxide oxidizes Fe^{2+} to Fe^{3+} and dissociates to a hydroxyl ion and a hydroxyl radical (Equation 1).[49] Active Fe^{2+} can be regenerated from Fe^{3+} by using a chemical reductive agent, such as ascorbic acid, or electrochemical reduction at the working electrode.[50, 51] Several other transition metal ions in their lower oxidation states (e.g. Cu^{+}, Ti^{3+}, Cr^{2+}, and Co^{2+}) and their complexes catalyze "Fenton-like" oxidation reactions similarly to the Fenton reagents.[22]

(1) $Fe^{2+} + H_2O_2 \rightarrow Fe^{3+} + OH^{\bullet} + OH^{-}$

Radiolysis of water and photolysis of hydrogen peroxide generate hydroxyl radicals photochemically. Radiolysis of water can be achieved by synchrotron X-ray irradiation,[52, 53] γ-ray irradiation produced by decay of, for example, ^{60}Co or ^{137}Ce,[11, 54] or pulsed electron beams accelerated in a particle accelerator.[55] The specific, expensive equipment, which is not widely accessible, and use of ionizing radiation are the disadvantages of the radiolytic techniques. UV-induced homolysis of hydrogen peroxide in an aqueous solution generates two hydroxyl radicals.[56] The advantage of photochemical methods is fast (nano- to microseconds) radical generation, which allows time-resolved protein footprinting.[47, 55]

Water can be oxidized in an electrochemical cell to hydroxyl radicals at sufficiently high potentials.[21] A high voltage (typically 6-8 kV) on the electrospray emitter tip of an ordinary electrospray ion source of a mass spectrometer can generate a corona discharge, which leads to formation of hydroxyl radicals and other ROS, which can react with proteins in the gas phase.[57] Oxygen can be used as a nebulizer gas to enhance formation of ROS.

Hydroxyl radicals react with organic molecules by hydrogen atom abstraction from saturated carbons or by addition to unsaturated bonds or aromatic rings.[22] Even though the hydroxyl radicals are relatively non-selective oxidants, the selectivity of their reactions is determined by several factors: the strength of the C-H bond, the electronegativity of the substituents on the target sites, the stability of the nascent organoradical, steric effects, and statistical factors (i.e. the number of equivalent positions of attack).[8, 22]

As proteins are the primary target of hydroxyl radicals in oxidative stress, oxidation of proteins, peptides, and amino acids by hydroxyl radicals has been widely studied.[11, 58-61] Hydroxyl radicals provide also an excellent tool for protein footprinting and enable investigations of protein structure, folding/unfolding, interactions, aggregation, and onset of oxidative damage.[47, 53, 56, 62-64] Hydroxyl radicals are able to oxidize both the backbone and the side chains of proteins, but the amino acid residues are usually more accessible than the backbone.[22] Cysteine and methionine are the amino acids most susceptible to hydroxyl radical attack, followed by the aromatic tryptophan, tyrosine, and phenylalanine.[8, 22, 58]

The hydroxyl radical-based Fenton reaction has sporadically been used for imitation of drug metabolism. Fenton reaction products of various compounds have been compared with the metabolites of these compounds reported in the literature.[27-29, 32-35] Fenton reaction was observed to imitate several metabolites resulting from, for instance, aliphatic, aromatic, and benzylic hydroxylation, dehydrogenation, N-dealkylation, S-oxidation, defluorination, and decarboxylation, and combinations of these (Table 1). Electrochemically assisted Fenton reaction (EC-Fenton) has been shown to imitate hydroxylation, dehydrogenation, and heteroatom oxidation and dealkylation metabolic reactions.[26] Detailed experimental comparisons of metabolic and Fenton reaction product profiles remain nevertheless

scarce.[26] Formation of reactive quinone metabolites and intermediate semiquinones of paracetamol,[65] amodiaquine,[66] and pyronaridine[67] have also been studied by electron pulse radiolysis.

1.3.2 Direct electrochemical oxidation

Direct electrochemical oxidation is initiated by electron abstraction from the substrate by the electrode, and thus, requires the presence of a non-binding electron that can be initially abstracted.[68] Therefore, the sulphur-containing cysteine and methionine, and aromatic tryptophan and tyrosine are the amino acids most susceptible to direct electrochemical oxidation.[21] Oxidation of cysteine and methionine is reversible, whereas oxidative modifications in tryptophan and tyrosine are irreversible. Electrochemical oxidation of tyrosine and tryptophan leads to protein cleavage at the C-terminal side of tyrosine and tryptophan.[69, 70] This has been suggested as an alternative to the traditional chemical and enzymatic cleavage methods, which cleave the proteins at specific amino acid residues. Enzymatic protein digestion methods are commonly used in bottom-up proteomics, where proteins are cleaved into smaller peptides for identification and characterization by MS.[71]

Interestingly, it was observed that phosphorylation of tyrosine prevents its electrochemical oxidation, inhibiting also the subsequent cleavage.[69] This has been exploited as an alternative way to distinquish between phosphorylated and unphosphorylated tyrosine residues in peptides.[72, 73] Identification of phosphorylation sites is a crucial task in phosphoproteomics.[71] Reversible phosphorylation of tyrosine, threonine, and serine is among the most important mechanisms in cell signaling.[74] Phosphorylation of tyrosine residues is involved in the regulation of various cellular processes such as proliferation, differentiation, cell cycle progression, cell adhesion, and metabolic homeostasis. Even though both phosphorylation and oxidation of proteins are well known, the effect of phosphorylation on oxidation of proteins and peptides has not been studied with methods involving biologically relevant ROS as oxidant species. Namely, the electron transfer mechanism of electrochemical oxidation may not be the most biologically relevant.

Imitation of the most important drug metabolism reactions and the compounds studied by direct EC have been reviewed recently.[68] In brief, direct EC has proved suitable for imitation of drug metabolism reactions that can begin with a single electron transfer mechanism, reactions such as dehydrogenation, S-oxidation, P-oxidation, and N-dealkylation (Table 1).[25] In addition, allylic,[36] benzylic,[26, 41] or aromatic hydroxylation[38, 40] as well as ipso-substitution[39, 42] can occur in EC if there is an activating electron-donating heteroatom substituent at a suitable position, enabling initial electron transfer followed by electron delocalization to the above-mentioned positions.[68] However, overoxidation is common in hydroxylation of substituted aromatic rings, as the hydroxylation products may be oxidized further at lower potentials than the starting compound.[25]

Even though, in principle, electrons can be abstracted from any bond, oxidation potentials of aliphatic hydrocarbons are typically higher than those of solvents.[75] Thus, aliphatic hydroxylation, aromatic hydroxylation of non-activated aromatic rings, and O-

dealkylation are not observed in direct electrochemistry.[25] However, aliphatic hydroxylation and aromatic hydroxylation reactions have been exceptionally achieved with use of a platinum electrode and 1.5–2 V potentials.[36, 37] The reaction is not direct EC, but is likely mediated by water oxidation (see Section 1.3.1 Hydroxyl radical-based methods).[37, 68] O-dealkylation was not achieved for 7-ethoxycoumarin,[25] but was reported for verapamil[41], metoprolol,[26] and toremifen[76] The mechanism was not discussed, however, and for verapamil and toremifen could actually be ipso-substitution. Electrochemical oxidation has resulted in product profiles very similar to those of *in vivo* and *in vitro* metabolism,[36] but also considerable differences have been reported.[26, 77]

1.3.3 Metalloporphyrins

Metalloporphyrins are metalloorganic complexes that act as surrogates for the active centers of CYP450 enzymes.[24] Metalloporphyrins have been widely used as biomimetic catalysts and for drug metabolism imitation. Whereas molecular oxygen is the oxygen donor in CYP450-catalyzed reactions,[78] single oxygen donors, such as peroxides, periodates, and iodosylbenzene, are used to provide the oxygen in metalloporphyrin reactions.[24] Iron and manganese are the most commonly used metals in metalloporphyrins. Different oxidants, solvents, and co-catalysts can be used to control the reaction.

Metalloporphyrins have been shown to be capable of imitating all of the common types of phase I drug metabolism reactions, including aliphatic, benzylic, and aromatic hydroxylation, N-dealkylation, O-dealkylation, N-oxidation, S-oxidation, and dehydrogenation (Table 1).[26] It is rare, however, that all of the main metabolites of a given drug could be imitated by metalloporphyrins.[79, 80] Comprehensive imitation of the metabolites of a selected drug may require using several different metalloporphyrin catalysts and reaction conditions.[81] The yields of the desired products can be low and byproducts, which are not observed in CYP450-mediated metabolism reactions, are often observed due to the different selectivities of metalloporphyrins and CYP450 reactions.[82-87] Controlling the orientation of the substrate respective to the metalloporphyrin may necessitate addition of binding groups to the substrate, especially in the oxidation of steroids.[88-91] Metalloporphyrins are strong oxidizing agents and easily oxidizable substrates can be overoxidized to stable products, thus bypassing possible reactive intermediates formed in phase I metabolism reactions.[24] However, careful selection and controlling of reaction conditions may also allow isolation of unstable metabolites or intermediates, which may not be observed in metabolism assays.[92] The production of the desired product in adequate amounts requires rigorous optimization of the reaction conditions such as selection of suitable metalloporphyrin and oxygen donor.[85] Nonetheless, even commercial kits for biomimetic production of drug metabolites are available.[93] Various reaction conditions are screened and then the reaction conditions are optimized for production of the desired metabolite.

1.4 Titanium dioxide photocatalysis

TiO_2 can catalyze both oxidation and reduction reactions when exposed to UV, which has higher energy than the band gap of TiO_2.[94] TiO_2 has three mineral forms: anatase, rutile, and brookite. Anatase and rutile are the most commonly used in photocatalysis and have band gaps of 3.2 eV (385 nm) and 3.0 eV (410 nm), respectively. Anatase is considered photocatalytically more active than rutile.[95-97] Commercial Degussa P25 TiO_2 is a mixture of anatase and rutile and exhibits higher photocatalytic activity than either anatase or rutile alone.[98]

UV excites electrons (e^-) from the valence band to the conduction band of TiO_2, leaving holes (h^+) on the valence band (Figure 1).[99] The formed electron–hole pair separates into a free electron and a free hole, which can diffuse to the surface of the TiO_2 particle. Surface-trapped holes can react with water to produce hydroxyl radicals or accept an electron directly from an organic molecule adsorbed onto the TiO_2 surface. Surface-trapped electrons can reduce molecular oxygen to superoxide. In addition, singlet oxygen can be formed by oxidation of superoxide by holes.[100, 101] However, singlet oxygen has a lifetime of 2 µs, and thus, is likely to participate in photocatalytic oxidation only if the molecule is adsorbed on the TiO_2 surface.[102, 103]

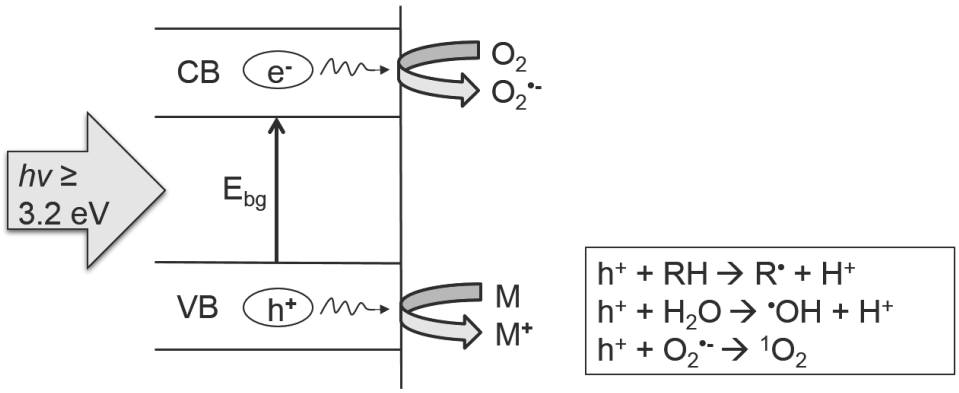

Figure 1 *The principle of TiO_2 photocatalysis (modified from [99, 104, 105]).*

The TiO_2 surface contains amphoteric titanol (TiOH) groups, and the point of zero charge of commercial Degussa P25 is 6.25.[105] Above pH 6.25, the TiOH groups deprotonate and the surface is negatively charged, whereas below pH 6.25, the TiOH groups protonate, making the surface charge positive. The enrichment of phosphopeptides using TiO_2 columns is based on this,[106-108] and pH control may be relevant also in photocatalytic oxidation experiments, even though inconsistent results of the effect of pH and adsorption of the substrate have been reported.[109-112]

TiO_2 photocatalysis has been widely applied to degradation of organic pollutants, waste water purification and self-cleaning materials.[94, 99, 104] In relation to oxidation of peptides

and proteins, TiO_2 photocatalysis has been proposed as an alternative protein and peptide digestion method[113] and used to study the byproducts of toxic microcystin peptides produced by cyanobacteria.[114, 115] As TiO_2 photocatalysis generates the same ROS as in biological systems, it provides a potential method for imitation of biological oxidation reactions in a pure matrix, free from biological interferences.

Previously, few studies have addressed the use of TiO_2 photocatalysis in imitation of drug metabolism,[30, 31, 44-46] and no experimental comparisons with other methods (such as EC and EC-Fenton) have been reported. TiO_2 photocatalysis was reported to be capable of hydroxylation, dehydrogenation, and N- and O-dealkylation, forming products similar to the metabolites formed *in vivo* and/or *in vitro* (Table 1).[30, 31, 44-46] The possible reaction mechanisms in TiO_2 photocatalysis, namely electron transfer on the TiO_2 surface or hydroxyl radical attack, should enable imitation of metabolism reactions beginning with electron transfer or hydrogen atom transfer mechanisms.

TiO_2 photocatalysis can be conventionally performed using micro- or nano-sized TiO_2 particles. However, the TiO_2 particles need to be removed before the analysis, which is time-consuming and can be difficult to assess by visual inspection in the case of micro- and nanoparticles. Performing photocatalysis on a TiO_2-coated surface eliminates this shortcoming. Photocatalytic coatings have been widely used in self-cleaning and antifogging materials such as windows and mirrors.[99] TiO_2 coating has also been utilized in a microchip that combined a TiO_2-coated nanoreactor and micropillar electrospray ionization (μPESI).[31] The microchip approach provided much faster analysis of photocatalytic reactions than conventional methods. However, the lack of separation of the possible reaction products is a disadvantage of this microchip. Furthermore, the fabrication of the μPESI chip is demanding and requires the use of expensive clean-room facilities.

1.5 Mass spectrometry in identification of reaction products

Reliable identification of reaction products requires specific and sensitive analytical methods. LC-MS offers excellent sensitivity and specificity and relatively high sample throughput for identification of unknown compounds. Since the invention of atmospheric ionization methods, LC-MS has become the preferred technique in drug metabolism and proteomics studies.[71, 116-118] The atmospheric ionization methods, electrospray ionization (ESI), atmospheric pressure chemical ionization, and atmospheric pressure photoionization, enable efficient ionization of different types of molecules and straightforward coupling of reversed phase LC to MS.[116, 117] ESI is a very soft ionization method, which also allows ionization of proteins and peptides as well as labile conjugates potentially formed in phase II metabolism.[116, 119] Ultra-high-performance LC (UHPLC) provides improved chromatographic resolution and decreased analysis time owing to the reduced particle size of stationary phases in UHPLC columns.[117]

Minimal sample preparation is preferred to avoid losing reaction products in pretreatment or causing conformation changes of proteins. For example, protein precipitation to stop the microsomal incubation is an adequate pretreatment in metabolite screening. Proteins can be analyzed as intact (top-down proteomics) or can be digested to

peptides prior to analysis (bottom-up proteomics).[71, 119] Reaction products are usually identified by comparing a test sample with a negative control (blank sample). Anticipated reaction products can be searched based on the change in the mass-to-charge ratio (*m/z*) (Table 2).[120] Various data mining tools, metabolite identification software, and protein sequence databases are used for identification of the reaction products.[117-120]

Table 2. *Examples of common phase I drug metabolism and protein oxidation reactions.*

	Reaction	Change in formula	Δ*m/z*
Phase I drug metabolism reactions[117]	Hydroxylation or heteroatom oxidation	+O	+16
	Hydroxylation+dehydrogenation (ketone formation)	+O-2H	+14
	Dehydrogenation	-2H	- 2
	Demethylation	$-CH_2$	-14
	Dihydroxylation	+2O	+32
Protein oxidation reactions[22]	Hydroxylation or methionine oxidation to sulfoxide	+O	+16
	Dihydroxylation, peroxidation, cysteine oxidation to sulfinic acid or methionine oxidation to sulfone	+2O	+32
	Trihydroxylation or cysteine oxidation to sulfonic acid	+3O	+48
	Hydroxylation+dehydrogenation (carbonylation)	+O-2H	+14
	Arginine deguanidination	$+O-CH_5N_3$	-43
	Glutamic or aspartic acid decarboxylation	$-CH_2O$	-30

High-resolution mass spectrometry

High-resolution mass spectrometry (HRMS) instruments, such as time-of-flight (TOF)-MS, orbitrap, and Fourier-transform ion synchrotron resonance, allow accurate mass measurement and high resolving power, i.e. the capacity to distinquish ions with close *m/z* values, enabling characterization and structural elucidation of unknown compounds.[121, 122] The elemental composition of an unknown compound can be calculated based on the accurate mass.[121] Mass accuracy is the difference between the theoretical (exact) and measured (accurate) mass of an ion. The higher the mass accuracy is, the fewer options of elemental compositions exist. High resolving power and the isotopic pattern fit increase certainty of the elemental composition calculation.[123] While HRMS allows distinguishing isobaric compounds, i.e. compounds with the same nominal mass but different exact masses, tandem mass spectrometry (MS/MS) is needed for distinguishing isomeric compounds, i.e. compounds having the same number of each isotopic atom but differing in their positions within the molecule.

Tandem mass spectrometry

MS/MS techniques provide structural information. Precursor ion and neutral loss scan modes of triple quadrupole instruments enable group-specific detection of unknown metabolites of a drug such as glucuronide or sulfate conjugates.[116, 117] In contrast, product ion scan is more powerful in structural characterization of the detected reaction products.[116] Determination of elemental compositions of product ions with exact mass measurements using HRMS instrument increases the certainty of structural characterization.[117] Typical hybrid instruments, which allow reproducible MS/MS with high resolution, have a quadrupole (Q) or an ion trap in front of HRMS, e.g. Q-TOF or ion trap-orbitrap.[120] MS^n experiments with an ion trap mass spectrometer enable more specific elucidation of the sites of modification, as the product ions can be selectively isolated and further fragmented.[116]

The N-terminal protein or peptide fragments are called a-, b-, and c-series and the C-terminal fragments x-, y-, and z-series, depending on the location of the bond cleavage.[71] The b- and y-series ions are most frequently observed ion types in low-energy collisions.[124] The amino acid sequence of the peptide and the sites of oxidative modifications can be deduced from the mass differences of fragment peaks observed in the product ion spectrum.

Ambient mass spectrometry

Ambient MS comprises methods enabling desorption and ionization of compounds directly on sample surfaces. The major advantage of these techniques is rapid analysis of the surfaces of native objects without the need for sample preparation.[125, 126] Thus, rapid screening and fingerprinting are major uses of these techniques, which can also be used in the field environment. A multitude of methods have been developed and examples include desorption electrospray ionization (DESI),[127] direct analysis in real time,[126] and desorption atmospheric photoionization.[128] DESI was used in this work for the sampling and ionization of photocatalytic oxidation products directly from a TiO_2-coated glass wafer.

In DESI, a pneumatically assisted charged spray is used to desorb and ionize compounds from a surface.[127] The solvent is sprayed from a small capillary with the aid of a nebulizer gas, typically nitrogen. Like in ESI, a potential difference of 1-8 kV is applied between the spray capillary and the mass spectrometer inlet. Desorption and ionization occur in a single step, likely by a droplet pick-up mechanism.[129-131] The spray droplets hit the sample, spreading out on the surface to form a thin liquid film, which then dissolves sample molecules. Later-arriving droplets remove the sample molecules from the surface. After desorption, the ionization proceeds as in ESI.[127] Multiple droplet fissions lead to formation of gas-phase analytes by ion evaporation[132, 133] or charge residue mechanisms,[134] and the ions are drawn into the mass spectrometer. Like ESI, DESI is best suited for ionic and polar compounds.

2 Aims of the study

Oxidative stress and ROS play an important role in several diseases. Therefore, it is important to develop methods to study ROS-mediated oxidation of biomolecules, as this can be difficult to investigate in the real biological environment. Radiolytic and photolytic methods used for the hydroxyl radical-based oxidation of proteins require the use of special equipment and/or ionizing radiation. TiO_2 photocatalysis may offer a more convenient way to oxidize biomolecules. In addition, the effect of tyrosine phosphorylation on oxidation of proteins, peptides, or amino acids has not been investigated by an oxidation method, where the oxidation is mediated by biologically relevant oxidant species, as in TiO_2 photocatalysis. Therefore, this study aimed at developing a TiO_2 photocatalytic method for oxidation of phosphopeptides and at applying it to examine the effect of phosphorylation on the oxidation of peptides using UHPLC-MS/MS for the analysis of reaction products (I).

Rapid, easy, and affordable methods are needed for screening and production of drug metabolites. Metalloporphyrins, EC, and Fenton reaction have not been able to imitate the oxidative phase I metabolism reactions adequately to allow comprehensive prediction of potential drug metabolites. A few studies have suggested that TiO_2 photocatalysis is a feasible method for drug metabolism imitation. However, the feasibility of TiO_2 photocatalysis for drug metabolism imitation has rarely been critically evaluated by comparing the photocatalytic reaction products with the actual metabolites using a proper UHPLC-MS/MS method that allows separation of potential isomeric products. Furthermore, experimental comparisons with other non-enzymatic oxidation reactions are completely lacking. To address this need, this work aimed at comparing the feasibilities of TiO_2 photocatalysis, EC, and EC-Fenton for imitation of phase I metabolism of drugs (II) and at evaluating the feasibility of TiO_2 photocatalysis for imitation of phase I metabolism of anabolic steroids (III) using UHPLC-MS/MS for the characterization of the reaction products. To enhance the applicability of TiO_2 photocatalysis for high-throughput screening of oxidation products, the aim was to develop a rapid and simple method for photocatalytic oxidation and mass spectrometric characterization of oxidation products by integrating TiO_2 photocatalysis with DESI-MS analysis (IV).

3 Experimental

This section briefly describes the chemicals, materials, samples, instrumentation, and experimental setups used in the work. Details can be found in original publications I-IV.

3.1 Chemicals and materials

Chemicals and materials used in the work are listed in Table 3. Notes indicate their use. The solvents were at least HPLC grade, and all reagents were at least reagent grade. Table 4 presents the model compounds used in this work.

Table 3. *Chemicals and materials used in the study.*

Chemical/Material	Manufacturer/Supplier	Use	Publication
Acetonitrile (ACN), LC-MS grade	Sigma-Aldrich (Steinheim, Germany)	Solvent	II-IV
Acetonitrile, HPLC grade	Biosolve BV (Valkenswaard, The Netherlands)	Solvent	II
Ammonium acetate	Sigma-Aldrich (Steinheim, Germany)	Reagent	II, III
Ammonium hydroxide	Mallinckrodt Baker B.V. (Denventer, The Netherlands)	Reagent	I
Androstenedione	Steraloids (Newport, RI, USA)	Standard	III
β-nicotinamide adenine dinucleotide 2′-phosphate reduced tetrasodium salt hydrate (NADPH)	Sigma-Aldrich (Steinheim, Germany)	Cosubstrate	II, III
Deionized water	Milli-Q Plus purification system (Molsheim, France), Arium® 611 (Sartorius Stedim Biotech Gmbh, Goettingen, Germany), and Millipore Elix® Essential 5 (Molsheim, France)	Solvent Solvent Reagent	I-IV II IV
Disodium hydrogen phosphate	Merck (Darmstadt, Germany)	Reagent	II, III
Ethylenediaminetetraacetic acid disodium salt dehydrate (EDTA, 99-101%)	Sigma-Aldrich (Steinheim, Germany)	Reagent	II

Table 3 continued *Chemicals and materials used in the study.*

Chemical/Material	Manufacturer/Supplier	Use	Publication
Ferric chloride hexahydrate (98%)	Sigma-Aldrich (Steinheim, Germany)	Reagent	II
Formic acid (98-100%)	Sigma-Aldrich (Steinheim, Germany)	Reagent	I, II, IV
Glacial acetic acid (≥ 99.85%)	Sigma-Aldrich (Steinheim, Germany)	Modifier	II, III
Human liver microsomes	BD Gentest (Franklin Lakes, NJ, USA)	Reagent	II, III
Magnesium chloride	Merck (Darmstadt, Germany)	Reagent	III
Magnesium chloride hexahydrate	Sigma-Aldrich (Steinheim, Germany)	Reagent	II
Methanol, LC-MS grade	Sigma-Aldrich (Steinheim, Germany)	Solvent	I-IV
Methanol, HPLC grade	Biosolve BV (Valkenswaard, The Netherlands)	Solvent	II
Oasis 30 mg 1 mL cartridges	Waters (Manchester, UK)	Solid phase extraction	III
Perchloric acid (70-72%)	Merck (Darmstadt, Germany)	Reagent	III
Pyrex glass wafer (diameter 100 mm, thickness 0.5 mm)	Plan Optik AG (Elsoff, Germany)	Sample platform	IV
Sodium dihydrogen phosphate	Sigma-Aldrich (Steinheim, Germany)	Reagent	II, III
Sodium hydroxide	Merck (Darmstadt, Germany)	Reagent	II, III
Titanium(IV) isopropoxide (TTIP) 97%	Aldrich (Steinheim, Germany)	Reagent	IV
TiO_2 Degussa P-25	Sigma-Aldrich (Steinheim, Germany)	Photocatalyst	I-III

Table 4. *Model compounds used in this work.*

Compound	Formula	$M_{monoisotope}$	Manufacturer/ Supplier	Publication
(Phospho)peptides (Insulin receptor peptide 1142-1153)				
TRDIYETDYYRK (IR0)	$C_{72}H_{107}N_{19}O_{24}$	1621.77	Anaspec	I
TRDIpYETDYYRK (IR1A)	$C_{72}H_{108}N_{19}O_{27}P$	1701.74	Anaspec	I
TRDIYETDpYYRK (IR1B)	$C_{72}H_{108}N_{19}O_{27}P$	1701.74	Anaspec	I
TRDIYETDYpYRK (IR1C)	$C_{72}H_{108}N_{19}O_{27}P$	1701.74	Anaspec	I
TRDIpYETDpYpYRK (IR3)	$C_{72}H_{110}N_{19}O_{33}P_3$	1861.67	Anaspec	I
Small drug molecules and anabolic steroids				
7-ethoxycoumarin	$C_{11}H_{10}O_3$	190.0630	Sigma-Aldrich	II
Amodiaquine dihydrochloride dihydrate	$C_{20}H_{22}ClN_3O$ (free base)	355.1451	Sigma-Aldrich	IV
D-amphetamine sulfate	$C_9H_{13}N$ (free base)	135.1048	Synthesized in house	IV
Atenolol	$C_{14}H_{22}N_2O_3$	266.1630	Sigma-Aldrich	IV
Buspirone hydrochloride	$C_{21}H_{31}N_5O_2$ (free base)	385.2478	Sigma-Aldrich	II, IV
Lidocaine hydrochloride monohydrate	$C_{14}H_{22}N_2O$ (free base)	234.1810	Sigma-Aldrich	IV
Metandienone	$C_{20}H_{28}O_2$	300.2089	Steraloids	III
Methyltestosterone	$C_{20}H_{30}O_2$	302.2246	Diosynth	III
Metoprolol tartrate	$C_{15}H_{25}NO_3$	267.1834	Sigma-Aldrich	IV
Moperone hydrochloride	$C_{22}H_{26}FNO_2$ (free base)	355.1948	Sigma-Aldrich	IV
Nadolol	$C_{17}H_{27}NO_4$	309.1940	Sigma-Aldrich	IV
Nandrolone	$C_{18}H_{26}O_2$	274.1933	Diosynth	III
Nicotine hydrogen tartrate	$C_{10}H_{14}N_2$ (free base)	162.1157	Sigma-Aldrich	IV
Quinidine sulfate dihydrate	$C_{20}H_{24}N_2O_2$ (free base)	324.2838	Sigma-Aldrich	IV
Stanozolol	$C_{21}H_{32}N_2O$	328.2515	Sterling-Winthorp	III
Promazine hydrochloride	$C_{17}H_{20}N_2S$ (free base)	284.1347	Sigma-Aldrich and Orion	II
Propranolol hydrochloride	$C_{16}H_{21}NO_2$ (free base)	259.1572	Sigma-Aldrich	IV
Testosterone	$C_{19}H_{28}O_2$	288.2089	Sigma-Aldrich	II, III
Verapamil hydrochloride	$C_{27}H_{38}N_2O_4$ (free base)	454.2832	Sigma-Aldrich	IV

T threonine, R arginine, D aspartic acid, I isoleucine, Y tyrosine, E glutamic acid, K lysine, p phosphorylated
Anaspec (Fremont, CA, USA), Sigma-Aldrich (Steinheim, Germany), Steraloids (Newport, RI, USA), Diosynth (Oss, The Netherlands), Orion (Orion Oy, Espoo, Finland)

3.2 Sample preparation

3.2.1 Titanium dioxide photocatalysis

Nanoparticle-based titanium dioxide photocatalysis

Photocatalytic reactions of (phospho)peptides (I), small drug and drug-like molecules (II), and anabolic steroids (III) were performed in duplicate using Degussa P25 TiO_2 nanoparticles. Blank samples were prepared without the substrate. The samples were magnetically stirred while exposed from above to a 5000-PC Series Dymax UV Curing Flood Lamp (Dymax Light Curing Systems, Torrington, CT, USA). The lamp was a metal halide UV lamp with nominal intensity of 225 mW cm^{-2}. The photocatalytic protocols for oxidation of (phospho)peptides, anabolic steroids, and drugs as well as for evaluation of the effect of acetonitrile on the photocatalytic reaction kinetics and routes are described in Table 5.

Titanium dioxide photocatalysis integrated with desorption electrospray ionization – mass spectrometry

The TiO_2-coated wafers were fabricated by depositing TiO_2 films on Pyrex glass wafers by atomic layer deposition (ALD) from TTIP and deionized water at a temperature of 250°C with Picosun^{TM} R-150 ALD reactor (Picosun Oy, Espoo, Finland). TTIP was evaporated from a heated source and water from an external vessel, held at 60°C and at room temperature, respectively. Reactor pressure was in the order of 5 mbar, maintained by mass flow controlled, constant nitrogen (99.999% N_2) flow and Adixen 2033 C2 vacuum pump (Adixen Vacuum Products, Annecy, France). Deposition sequence of 1.6 s TTIP pulse, 5 s purge, 0.1 s water pulse, and 5 s purge was repeated for 4000 cycles. The TiO_2 films were characterized by UV-VIS reflectometry (Hitachi U-2000, Hitachi Ltd., Tokyo, Japan) and X-ray diffraction (PANalytical X'Pet Pro, Cu Kα radiation, PANalytical B.V., Almelo, The Netherlands).

Aqueous samples (1 μL) of the model drug compounds (50 μM or 100 μM) were dispensed on the rim of the TiO_2-coated wafer. The diameter of a sample spot was about 2.5 mm and the sample spots were about 1 mm apart from each other. The sample spots were UV exposed (for 15-180 s) from above either online or offline. The UV-exposed droplets were allowed to evaporate before DESI-MS analysis.

Offline reactions were performed using a 5000-PC Series Dymax UV Curing Flood Lamp with a metal halide lamp. The whole TiO_2-coated wafer was placed under the UV lamp (distance approximately 15 cm). For online reactions, a UV lamp (TEK-Lite, Union Bridge, MD, USA, maximum at peak 365 nm, intensity of 100 mW cm^{-2}) was positioned 3.5 mm above the sample wafer. The samples were UV exposed while the TiO_2-coated wafer rotated and transferred the exposed samples online to DESI-MS analysis.

Table 5. *Photocatalytic reaction conditions using TiO_2 nanoparticles.*

	(Phospho-) peptides (I)	Studying the effect of ACN (II & III)	Drugs (II)	Anabolic steroids (III)
Volume of reaction mixture	100 µL	500 µL	500 µL	500 µL
TiO_2 concentration	0.1 g L^{-1}	1 g L^{-1}	1 g L^{-1}	1 g L^{-1}
Substrate concentration	100 µM	10 µM	10 µM	10 µM
Solvent	0.01% ammonium hydroxide	0%, 1%, & 50% ACN (buspirone) 1%, 50% & 95% ACN (testosterone)	Water (buspirone and promazine) or 1% ACN (7-ethoxycoumarin and testosterone)	1% ACN, except for stanozolol 50% ACN
Duration of UV exposure	0, 2, 4, 6, 8, 10, and 15 min	0, 15, 30, 45, 60, 90, and 120 s (0% ACN) 0, (0.5) 1, 2, 3, 4, 6, and 12 min (1% ACN) 1, 5, 10, 15, 20, and 30 min (50% & 95% ACN)	15 s (buspirone and promazine) or 2 min (7-ethoxycoumarin and testosterone)	2 min, except for stanozolol 15 min
Removal of TiO_2 particles by 10-min centrifugation at 13200 rpm				
Supernatant 1.	90 µL	470 µL	470 µL	470 µL
Centrifugation of first supernatant for 10 min at 13200 rpm				
Supernatant 2.	72 µL	450 µL	450 µL	450 µL
Pretreatment of supernatant 2.	Addition of 8 µL of methanol	No pretreatment	No pretreatment, except 9-fold enrichment for 7-ethoxycoumarin and testosterone for acquisition of the product ion spectra of the photocatalytic products	Solid-phase extraction (3.2.5)

3.2.2 Incubation of human liver microsomes

The phase I metabolism reactions of buspirone, promazine, testosterone, and 7-ethoxycoumarin (II) as well as metandienone, methyltestosterone, nandrolone, stanozolol, and testosterone (III) were performed *in vitro* with HLMs (Table 6).

Table 6. *Human liver microsomal incubation protocols.*

	Drugs (II)	**Anabolic steroids (III)**
Total volume	100 µL	100 µL
Phosphate buffer concentration (pH 7.4)	50 mM	50 mM
Substrate concentration	50 µM	50 µM
Substrate solvent	water (buspirone and promazine), water–acetonitrile (testosterone and 7-ethoxycoumarin)	acetonitrile (testosterone, methyltestosterone, metandienone, and nandrolone) or methanol (stanozolol) solution
Final concentration of organic solvent	0.5%	1%
$MgCl_2$ concentration	5 mM	5 mM
Initiation	5 µL of 20 mM NADPH	5 µL of 20 mM NADPH
Cosubstrate addition	-	5 µL of 20 mM NADPH at 6, 12, and 18 h
Incubation time	2 h	1, 3, 6, 12, 18, and 24 h
Termination by protein precipitation	200 µL ice-cold acetonitrile, and transfer of the tubes to -18 °C for 30 min	10 µL 4 M perchloric acid, and transfer of the tubes into an ice bath
Removal of precipitated HLMs	centrifugation at 13200 rpm for 10 min	centrifugation at 13200 rpm for 10 min
Pooling	-	supernatants from 1, 3, 6, 12, 18, and 24 h incubations
Pretreatment	-	Solid-phase extraction (see Section 3.2.5)

3.2.3 Electrochemical oxidation

The test solution contained 10 µM buspirone, promazine, testosterone, or 7-ethoxycoumarin in acetonitrile:water 50:50 + 0.1% formic acid (EC-acidic). In the case of testosterone and 7-ethoxycoumarin, no products were observed at 10 µM concentration and the concentration was increased to 100 µM. Also basic conditions (EC-basic) were tested for the oxidation of

buspirone and promazine, with acetonitrile:water 50:50 + 0.1% ammonium hydroxide used as the solvent. The solution was infused at a flow rate of 50 µL min^{-1} through the electrochemical ESA 5021A conditioning cell with a working electrode of porous graphite (ESA Inc., Bedford, MA, USA). The electrochemical cell was controlled by an ESA Coulochem III potentiostat (ESA Inc.). All reported cell potentials are versus a palladium reference electrode. The potential was ramped from 0 to 1500 mV with steps of 10 mV / 3.6 s. All the potential ramp experiments were made in duplicate. Online-ESI-MS was used to monitor the formed products. Samples for UHPLC-MS analysis were collected at constant potentials chosen on the basis of the potential ramp experiments (Table 7). The samples were diluted 10-fold with water before UHPLC-MS analysis.

Table 7. *Constant potentials used for sample collection in direct EC.*

Compound	EC-acidic, potential (mV)	EC-basic, potential (mV)
Buspirone	800, 1000, 1200, 1500	800, 1000, 1200, 1500
Promazine	500, 600, 1000, 1200, 1500	600, 700, 800, 1000
Testosterone and 7-Ethoxycoumarin	No products observed in ramps in acidic conditions → no sample collected with constant potentials	

3.2.4 Electrochemically assisted Fenton reaction

The EC-Fenton setup used for buspirone, promazine, testosterone, and 7-ethoxycoumarin (II) was based on the methods previously reported.[26, 51] Each reaction mixture (550 µL) consisted of 50 µL 10 mM substrate (in water or acetonitrile), 50 µL 10 mM EDTA/$FeCl_3$ in water, 125 µL or 75 µL acetonitrile, 275 µL or 325 µL water (depending on whether the sample was in water or acetonitrile, respectively) and 50 µL 0.1 M hydrogen peroxide (added just before the start of infusion through the EC cell). An ESA 5021A conditioning cell with a working electrode of porous graphite was used for EC-Fenton reactions. Samples were infused through the electrochemical cell first at a flow rate of 50 µL min^{-1}. After 1 min, the flow rate was lowered to 2 µL min^{-1} and a potential of -500 mV was applied. Sample collection was started after 15 min. The samples were diluted 25-fold with water before UHPLC-MS analysis.

3.2.5 Solid-phase extraction

For the anabolic steroids (III), the second supernatant (450 µL) of photocatalytic reactions and the pooled supernatant (270 µL) from HLM incubations, used for comparison of the reaction products, were diluted each with 1 mL of 100 mM ammonium acetate buffer (pH 6.0) for solid-phase extraction. Waters Oasis 30 mg 1 mL cartridges were conditioned with 1 mL of methanol and 1 mL of purified water. The sample was loaded to the cartridge, which was then washed with 1 mL of water-methanol 95:5 (v:v) and 1 mL of water-methanol 95:5 (v:v) + 2% acetic acid. The steroids and reaction products were eluted from

the cartridge with 1.5 mL of acetonitrile (testosterone, methyltestosterone, metandienone, and nandrolone) or 1.5 mL of methanol (stanozolol). The samples were evaporated to dryness in a water bath under nitrogen. Dry residues were reconstituted in 100 µL (HLM samples) or 50 µL (photocatalysis samples) of the LC mobile phase A:B 75:25 (v:v) (Table 8).

3.3 Analytical methods and instrumentation

3.3.1 Liquid chromatography – mass spectrometry

ACQUITY UPLC™ (Waters, Milford, MA, USA) and Xevo™ Q-TOF-MS (Waters, Manchester, UK) were used for analysis of the reaction products of (phospho)peptides (I), small drug molecules (II), and anabolic steroids (III) (Table 8). The chromatographic gradients were optimized for each model compound and details can be found in the original publications (I-III). MS and MS/MS spectra were collected in the positive ion mode using electrospray ionization (ESI). MS data were centroided and corrected during acquisition using as external reference (Lockspray) leucine enkephalin (concentration 2 ng μL^{-1}, flow rate 20 µL min^{-1}) at *m/z* 556.2771.

Metabolynx XS V4.1 software (Waters, Milford, MA, USA) was used in the search for unexpected reaction products (II, III). If a reaction product with the same *m/z* and retention time (t_R) as in HLM experiments was found also in TiO_2 photocatalytic reactions, electrochemical oxidation, or Fenton reaction, its product ion spectrum was compared with the product ion spectrum of the corresponding metabolite (see Table 8 for criteria).

A TSQ Quantum AM (Thermo Fisher Scientific, Waltham, MA, USA) triple quadrupole mass spectrometer was used for online monitoring of products during EC potential ramps. The detailed parameters can be found in the original publication (II).

Table 8. *Parameters used for detection of the model compounds and their reaction products with UHPLC–ESI–Q-TOF-MS.*

Parameter	(Phospho)peptides (I)			Buspirone and testosterone (II)	Promazine and 7-ethoxycoumarin (II)	Anabolic steroids (III)
Chromatographic parameters						
Column	Acquity UPLC BEH C-18 column (100 mm x 2.1 mm i.d., 1.7 µm particle size)					
Precolumn	Vanguard BEH C18 (5 mm x 2.1 mm i.d., 1.7 µm particle size)			in-line filter (0.2 µm) or Vanguard BEH C18	in-line filter (0.2 µm)	Vanguard BEH C18
Eluent A	0.1% formic acid			95:5 water/100 mM ammonium acetate		
Eluent B	0.1% formic acid in methanol/water 98:2			95:5 methanol/100 mM ammonium acetate		
Buffer pH (adjusted with acetic acid)	n/a			4.5 or 6.0	4.5	6.0
Injection volume and mode	5 µL, partial loop			5 µL, partial loop	5 µL, partial loop	5 µL, partial loop
Sample and column temperature	8°C, 40°C			8°C, 40°C	8°C, 40°C	8°C, 40°C
Mass spectrometric parameters	IR0	IR1A, IR1B, IR1C				
Capillary voltage (kV)	3	3	4	3	3	3
Extraction cone voltage (V)	0	0	0	3	3	3
Sampling cone voltage (V)	20	20	45	25	20	25
MS scan range (*m/z*)	400–1650	400–1750	400–1900	30–560	30–560	30–560
Product ion scan range (*m/z*)	70–1650	70–1750		30–560	30–560	30–560
Scan time (s)	0.15	0.15	0.15	0.1	0.1	0.1
Ion source temperature	150°C			150°C	150°C	120°C
Desolvation gas (nitrogen)	1000 L h^{-1}, 500°C			1000 L h^{-1}, 500°C	1000 L h^{-1}, 500°C	800 L h^{-1}, 450°C
Collision energy (eV) (Collision gas argon)	25			30 (buspirone) 25 (testosterone)	20 (promazine) 25 (7-ethoxy-coumarin)	15 & 20 (metandienone) 20 & 25 (methyl-testosterone and nandrolone), 42 & 47 (stanozolol) 20 & 30 (testosterone)
Criteria for reaction products with matching *m/z* and t_R selected for comparison of product ion spectra						
Mass window				30 ppm	30 ppm	20 ppm
t_R window				0.05 min	0.05 min	0.5%

3.3.2 Desorption electrospray ionization – mass spectrometry integrated with titanium dioxide photocatalysis

In DESI-MS, a home-built sprayer was used with Agilent Ion Trap 6330 (Agilent Technologies, Walbronn, Germany) in the positive ion mode (Figure 2). The ESI capillary (i.d. 83 µm, o.d. 184 µm) was grounded and the MS inlet capillary voltage was 2000 V. Nebulizer gas (N_2) was introduced at 9.5 bar through the outer capillary (i.d. 0.25 mm). The sprayer was attached to an x-, y-, z-stage, aligned parallel to the MS inlet, on-axis, with the following geometry: impact angle ~60°, vertical distance from sprayer to sampling surface ~4 mm. The sampling surface was level with the lower edge of flared capillary extension inlet (i.d. 1.6 mm). The horizontal distance of the sample to the MS inlet was ~10 mm. Methanol/water (1:1, v:v) + 0.1% formic acid was used as the spray solvent at the flow rate of 3 µL min^{-1}. The TiO_2-coated glass wafer used as a sampling surface was placed on a rotating platform (Thorlabs CR1-Z7/M, Thorlabs Sweden AB, Gothenburg, Sweden), which was placed on an x-, y-, z-stage. The rotation of the platform was controlled by Thorlabs computer software APT motor controller.

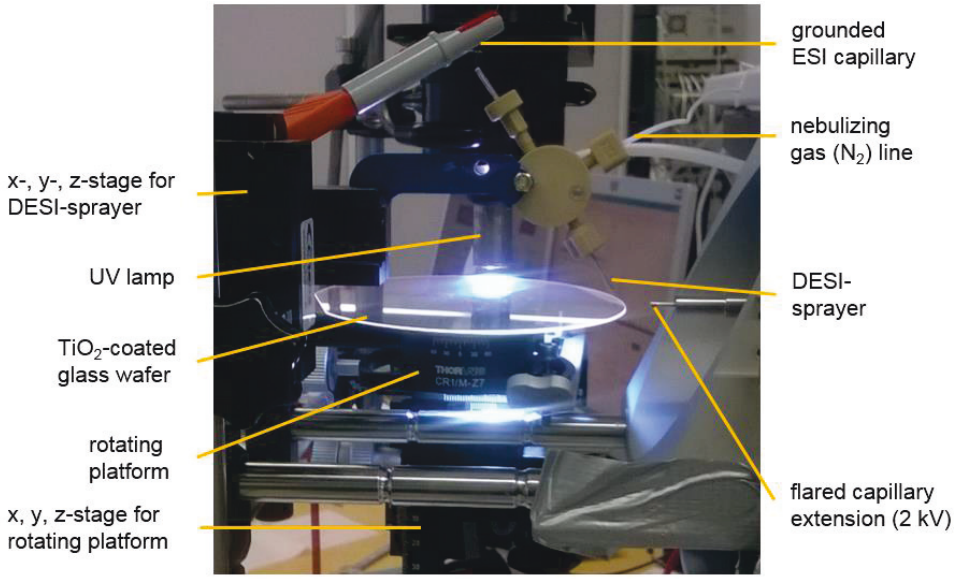

Figure 2 *TiO_2 photocatalysis–DESI-MS rotating array platform setup.*

4 Results and discussion

4.1 Photocatalytic oxidation of phosphopeptides

As phosphorylation of the tyrosine residue has a key role in the cellular processes, its effect on the oxidation process mediated by ROS was addressed in this study (I). A TiO_2 photocatalytic oxidation method was developed to compare the effect of phosphorylation with the help of five peptides, which had the same sequence (TRDIYETDYYRK), and three tyrosine (Y) residues of which none (IR0), all (IR3), or one was phosphorylated (IR1A, IR1B, and IR1C). UHPLC-ESI-MS methods were developed for the analysis of reaction products.

4.1.1 Optimization of duration of exposure to ultraviolet radiation

First, the duration of the UV exposure for the TiO_2 photocatalytic oxidation of the studied (phospho)peptides was optimized. The peptides decomposed under TiO_2 photocatalysis within 15 min (Figure 3). The initial, but not always the most abundant, oxidation products were M+O and M+2O products, on which this study concentrated. All initial oxidation products of each peptide formed and degraded following similar kinetics. The UV exposure time yielding the greatest abundance of M+O and M+2O products was chosen for the structural elucidation of the M+O and M+2O products (Figure 3), and was 2 min for IR1A and IR1C, 4 min for IR0, and 6 min for IR1B. The UV exposure time was not optimized for IR3, as no oxidation products were observed with UV exposure time of either 1 min or 6 min.

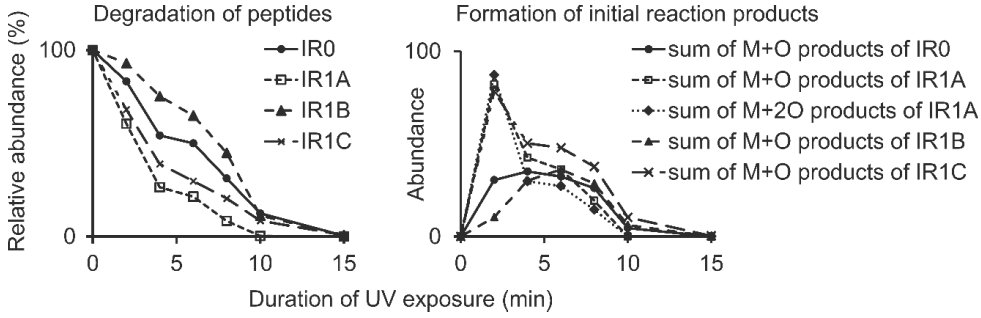

Figure 3 *Degradation of peptides IR0, IR1A, IR1B, and IR1C and formation of initial reaction products under TiO_2 photocatalysis (calculated using the triply protonated ion).*

4.1.2 Identification of photocatalytic oxidation products of (phospho)peptides

The mass spectra of peptides IR0, IR1A, IR1B, IR1C, and IR3 analyzed by the developed UHPLC-ESI-MS method showed multiple protonated molecules (one to four protons). The triple protonated molecule $[M+3H]^{+3}$ was the most abundant ion for nearly all peptides and their M+O and M+2O oxidation products. Thus, it was selected as the precursor ion for product ion analyses. The most common product ions of the peptides were sequence diagnostic single protonated N-terminal b-ions and C-terminal y-ions. The oxidation sites of the M+O and M+2O products of the studied peptides were determined based on the oxidized and the nonoxidized b- and y-ions of the peptides (Table 9). As an example, the product ion spectrum of the M+O product of IR0 eluting at 1.90 min showed an oxidized y_4-ion and a nonoxidized y_3-ion, indicating that the oxidation site was Y9. Similar data interpretation also applies to the other identifications.

TiO_2 photocatalysis produced five M+O products of IR0, eight M+O and five M+2O products of IR1A, two M+O products of IR1B, and five M+O products of IR1C (Table 9). Traces of M+2O products of IR0, IR1B, and IR1C were also observed, but at quantities lower than those needed for reliable identification based on acquisition of the product ion spectra. By considering all oxidation products, the oxidation site was at a nonphosphorylated tyrosine (Y) in 21 products, at a phosphorylated tyrosine in two products, and at isoleucine 4 (I4) in two products. Thus, the nonphosphorylated peptide IR0 and the monophosphorylated peptides IR1A, IR1B, and IR1C were preferentially oxidized at nonphosphorylated tyrosines. This is in agreement with the reaction rate constant of tyrosine with hydroxyl radicals, which is at least an order of magnitude higher than that of the other amino acids present in the studied peptides.[22] The two observed M+2O products of isoleucine (based on diagnostic b_4+2O ion) are consistent with the reaction rate constant of hydroxyl radicals with isoleucine (1.8×10^9 $M^{-1}s^{-1}$), being the third highest after tyrosine and arginine, and approximately an order of magnitude higher than those of the other amino acids (7.5×10^7–5.1×10^8 $M^{-1}s^{-1}$) present in the studied IR peptides.[22] Interestingly, both oxygens in the M+2O oxidation products attacked the same amino acid.

Although the favored oxidization site was shown to be at a nonphosphorylated tyrosine, IR1A and IR1C each produced a minor M+O product, in which the oxidation site was the phosphorylated tyrosine. However, no oxidation products of the triply phosphorylated peptide IR3 (all tyrosines phosphorylated: pY5, pY9, and pY10) were observed. Thus, the results suggest that phosphorylation of tyrosine significantly inhibits its oxidation under TiO_2 photocatalysis conditions.

Table 9. *Proposed diagnostic product ions of the reaction products. Accurate masses of the precursors and product ions can be found in the Supporting Information of original publication I.*

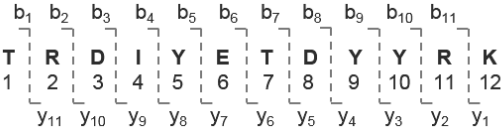

Nonoxidized product ions are marked with X, singly oxidized product ions (X+O) are marked with O, and doubly oxidized product ions (X+2O) are marked with 2O.

Pept./ prod.	Oxidation site	t_R (min)	Prec. $[M+3H]^{3+}$	b_4	b_5	b_6	y_3	y_4	y_5	y_6	Other[c]
IR0	-	5.98	541.6	X	X	X	X	X	X	X	
M+O	Y9	1.90	546.9	X	X	X	X	O	O	O	
M+O	Y10*	2.42	546.9	X	X	X	O	O	O	O	
M+O	Y5	4.31	546.9	X	O	O	X	X	X	X	
M+O	Y9 & Y10[a*]	4.57	546.9	X	X	X	X/O	O	O	O	
IR1A	-	5.43	568.3	X	X	X	X	X	X	X	
M+O	Y9	2.09	573.6	X	X	X	X	O	O	O	
M+O	Y9 & Y10[a*]	2.29	573.6	X	X	X	X/O	O	O	O	
M+O	Y9 & Y10[a*]	2.57	573.6	X	X	X	X/O	O		O	
M+O	Y9 & Y10[a*]	4.00	573.6	X	X	X	X/O	O	O	O	
M+O	pY5	7.00	573.6	X	O	O	X	X	X	X	
M+2O	Y9	2.62	578.9	X	X	X	X	2O	2O	2O	
M+2O	I4	2.94	578.9	2O	2O	2O	X	X	X	X	b_3
M+2O	Y10	3.13	578.9	X	X		2O	2O	2O		x_2
M+2O	Y9[b]	3.30	578.9	X	X	X					b_8, z_3
M+2O	I4	3.67	578.9	2O			X	X	X	X	b_3
IR1B	-	9.64	568.3	X	X	X	X	X	X	X	
M+O	Y5	7.42	573.6	X	O	O	X	X	X	X	
M+O	Y10*	7.57	573.6	X	X	X	O		O	O	
IR1C	-	5.20	568.3	X	X	X	X	X	X	X	
M+O	Y9	1.94	573.6	X	X	X	X	O	O	O	
M+O	Y9	2.14	573.6	X	X	X	X	O	O	O	
M+O	Y5	3.61	573.6	X	O	O	X	X	X	X	
M+O	Y9	3.80	573.6	X	X	X	X	O	O	O	
M+O	pY10*	8.29	573.6	X	X	X	O	O	O	O	

[a]Two oxidation products that could not be resolved chromatographically.

[b]No oxidized product ions were observed, but the nonoxidized product ions rule out there being other oxidation sites.

[c]Other diagnostic product ions (nonoxidized).

*y_1- and y_2-ions were not observed in the product ion spectra, and hence, the assignment of the oxidation site is not explicit. Y10 was assumed to be more readily oxidized than arginine 11 (R11) or lysine 12 (K12), as the reaction rate of hydroxyl radicals with Y (1.3×10^{10} $M^{-1}s^{-1}$) is approximately an order of magnitude higher than with R (3.5×10^{9} $M^{-1}s^{-1}$) and two orders of magnitude higher than with K (3.5×10^{8} $M^{-1}s^{-1}$).[22]

Pept. *peptide,* prod. *product,* Prec. *precursor ion*

The two products in which the oxidation site was a phosphorylated tyrosine eluted later in the reversed-phase C18 liquid chromatography conditions than did the respective nonoxidized peptide (Table 9). Instead, the M+O and M+2O products in which the oxidation occurred at a nonphosphorylated tyrosine eluted earlier than the respective nonoxidized peptides. Thus, oxidation of the phosphorylated tyrosine rendered the peptide more hydrophobic, increasing its retention within the C18 column, whereas oxidation at a nonphosphorylated tyrosine yielded more polar products, with decreased retention relative to the respective nonoxidized peptide. Hydroxylation of a phosphorylated tyrosine may enable internal hydrogen bonding between the formed hydroxyl group and the phosphate group, thus rendering the peptide more hydrophobic (Figure 4).

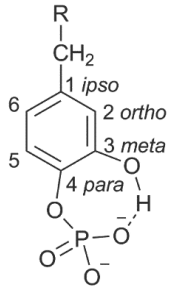

Figure 4 *Internal hydrogen bonding may cause the increased hydrophobicity of the peptide oxidized at the phosphorylated tyrosine.*

4.1.3 Mechanism of photocatalytic oxidation of (phospho)peptides

The possible oxidant species involved in TiO_2 photocatalysis include the hole on the TiO_2 surface, the hydroxyl radical, the superoxide ion, and the singlet oxygen.[99] In addition, hydrogen peroxide and molecular oxygen are involved in the photocatalytic oxidation reactions. The reaction rate of hydroxyl radical with tyrosine (1.3×10^{10} $M^{-1}s^{-1}$)[22] is significantly higher than those of either the superoxide ion or the singlet oxygen ($1.0\pm0.2\times10^{1}$ $M^{-1}s^{-1}$ and $0.8–0.9\times10^{7}$ $M^{-1}s^{-1}$, respectively).[10] Moreover, the oxidation of tyrosine residue is more likely to be mediated by hydroxyl radicals than by surface holes since basic reaction conditions (pH 10.5) were chosen to prevent the adsorption of the peptides onto the TiO_2 surface. At this pH, the TiO_2 surface is negatively charged[105] and electrostatic repulsion orients the negatively charged phenolic moiety of the tyrosine residue and the negatively charged phosphate group at the phosphorylated tyrosine out from the TiO_2 surface, which results in decreased interaction and oxidation of tyrosine residues of the peptides with the holes. It has also been suggested that organic molecules should be adsorbed onto the TiO_2 surface[103] to react with the short-lived singlet oxygen (lifetime 2-3 μs).[102] Hence, hydroxyl radicals obviously play a major role in initiating oxidation reactions of the tyrosine residue of the studied peptides.

Xu and Chance presented a scheme for a hydroxyl radical-initiated oxidation mechanism of tyrosine residue[22] in which the hydroxyl radical reacts rapidly with the tyrosine residue

that produces the dihydroxycyclohexadienyl radical (Figure 5). The most obvious reaction site is the *meta*-position, due to the directing effect of the original hydroxyl substituent at the *para*-position. The dihydroxycyclohexadienyl radical then reacts with oxygen (*via* addition), followed by the elimination of the hydroperoxyl radical to form α-hydroxycyclohexadienone, which is finally converted to 3,4-dihydroxyphenylalanine residue (DOPA) (M+O product). Further hydroxylation of DOPA *via* the same oxidation mechanism can produce trihydroxyphenylalanine residue (M+2O product). The inhibitory effect of phosphorylation upon the oxidation of tyrosine may be explained by the presented oxidation mechanism. The phosphorylation of the hydroxyl group of tyrosine (*para*-position) prevents the formation of the α-hydroxycyclohexadienone intermediate, and thus, inhibits oxidation of phosphorylated tyrosine. Even if the two *meta*-positions of each tyrosine are the favored oxidation sites, our results suggest that oxidation may also occur at other positions since four different M+O products of IR1A were oxidized at Y9, three different M+O products of IR1A were oxidized at Y10, and three different M+O products of IR1C were oxidized at Y9. However, the exact oxidation site at tyrosine was not elucidated in this study.

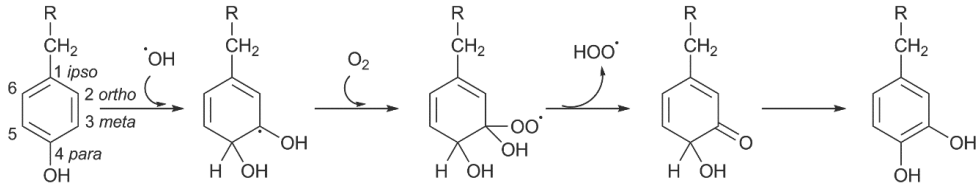

Figure 5 *Hydroxyl radical-mediated oxidation of tyrosine (adapted from [22]).*

4.2 Imitation of phase I metabolism by titanium dioxide photocatalysis

First, the TiO_2 photocatalytic reaction conditions were optimized for oxidation of small drug molecules with different polarities using buspirone and testosterone as model compounds (II, III). The feasibility of TiO_2 photocatalysis for imitation of phase I metabolism was compared with that of EC-Fenton and direct EC (II). Buspirone, promazine, testosterone, and 7-ethoxycoumarin were chosen as test compounds as their metabolism covers the most common phase I reactions such as aliphatic hydroxylation, aromatic hydroxylation, N-oxidation, S-oxidation, N-dealkylation, and O-dealkylation. The reaction products from TiO_2 photocatalysis, EC-Fenton, and direct EC reactions were compared with the phase I metabolites produced *in vitro* by human liver microsomes. The feasibility of TiO_2 photocatalysis for imitation of phase I metabolism of anabolic steroids was studied by comparing the photocatalytic reaction products of metandienone, methyltestosterone, nandrolone, stanozolol, and testosterone to the *in vitro* phase I HLM metabolites (III). UHPLC-ESI-MS methods were developed for the analysis of reaction products (II, III).

4.2.1 Optimization of photocatalytic reaction conditions

In TiO_2 photocatalysis, addition of organic solvent to water was necessary in order to increase the solubility of anabolic steroids and 7-ethoxycoumarin. Acetonitrile was selected as an organic solvent because it has weaker radical scavenging activity than methanol[135] The effect of acetonitrile on the photocatalytic oxidation reaction rates and routes was studied using three different solvent conditions per compound: 100% water, 1% and 50% acetonitrile in water were used for buspirone (II), whereas 1%, 50%, and 95% acetonitrile in water were used for testosterone (III).

The reaction products formed very fast in 100% water, and the intensity of the main products of buspirone was highest at 15 s (Figure 6). At longer UV exposure times, the initial products underwent further reaction or degradation. Acetonitrile effectively slowed down the photocatalytic reactions even at 1% concentration, and the highest intensity of the main products was observed at 2 min. The effect was even more pronounced at 50% and 95% concentrations of acetonitrile. At 50% acetonitrile concentration, the intensities of the products continuously increased within the 30-min time-frame studied. In 95% acetonitrile, however, the formation of the products became slower than their degradation by the end of the 30-min period.

Acetonitrile scavenges hydroxyl radicals,[135] which slows down the hydroxyl radical-mediated photocatalytic reaction. Acetonitrile was found not only to inhibit but also to direct the photocatalytic reactions; the increase of acetonitrile concentration completely inhibited a few of the products formed at the lowest acetonitrile concentration (buspirone 0%, testosterone 1%) (Figure 7). In addition, completely new products not observed at the lowest acetonitrile concentration were formed with increasing acetonitrile concentration (Figure 7). Detailed lists of the reaction products can be found in original publications II (buspirone) and III (testosterone). The reaction products of buspirone in 100% water and testosterone in 1% acetonitrile were similar to those described in Sections 4.2.2 and 4.2.3, even though not all the isomeric compounds were separated in the reaction condition optimization phase.

The increase of acetonitrile concentration also changed the relative abundances of the reaction products. As an example, 100% water favored formation of a hydroxylation+dehydrogenation product (M+O-2H, *m/z* 400, t_R 4.51 min) of buspirone over the formation of dehydrogenation (M-2H, *m/z* 384, t_R 5.47 min) and N-,N-deethylenation (M-C_2H_2 *m/z* 360, t_R 4.45 min) products (Figure 6). Increasing acetonitrile concentration clearly inhibited formation of the M+O-2H product and favored formation of the M-2H and M-C_2H_2 products of buspirone. In the case of testosterone, the same products were observed in 1% and 50% acetonitrile (Figure 7), although their relative intensities were different. Acetonitrile concentrations of 50% and 95% clearly favored the formation of a dehydrogenation product (M-2H, *m/z* 287.20, t_R 3.34 min) over the formation of hydroxylation (M+O, *m/z* 305.21, t_R 2.99 min) and hydroxylation+dehydrogenation (M+O-2H, *m/z* 303.19, t_R 2.67 min) products, whereas these three product types were formed with relatively similar abundances in 1% acetonitrile (Figure 6). In general, the formation of M+O and M+O-2H products was less abundant and slower in 95% acetonitrile than in 50% acetonitrile. The addition of acetonitrile, having electron scavenging capability, inhibited formation of ROS, and thus, formation of hydroxylation products. Therefore, at higher acetonitrile concentrations buspirone and testosterone instead reacted directly with the

photogenerated holes on the TiO_2 surface *via* one electron oxidation to produce dehydrogenation and, in the case of buspirone, N-dealkylation products.

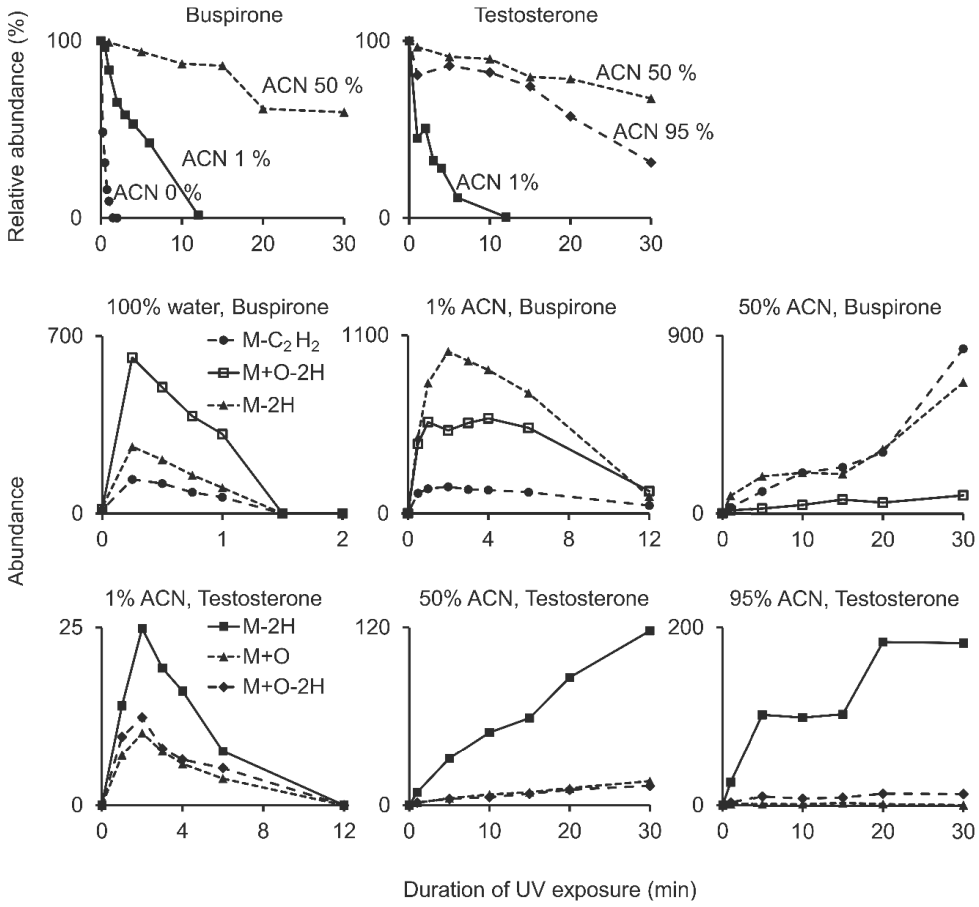

Figure 6 *Degradation of buspirone and testosterone and formation of selected reaction products in TiO_2 photocatalysis.*

Higher acetonitrile percentages with longer UV exposure times produced greater abundance of oxidation products in most cases (Figure 6). This is probably due to the slower degradation of formed products and may be useful in photocatalytic synthesis of metabolite standards. The possibility to use acetonitrile as a solvent enables oxidation of very poorly water-soluble compounds by TiO_2 photocatalysis. However, the amount of acetonitrile was kept to a minimum in this study in order to simulate physiological conditions and because the reactions were much faster and more convenient than with higher acetonitrile percentage. Thus, UV exposure times of 15 s and 2 min were chosen for TiO_2 photocatalysis in 100% water (buspirone and promazine) and 1% acetonitrile (metandienone, methyltestosterone, nandrolone, testosterone, and 7-ethoxycoumarin), respectively.

Stanozolol was not soluble enough in 1% acetonitrile, and thus, 50% acetonitrile and UV exposure time of 15 min were chosen for stanozolol.

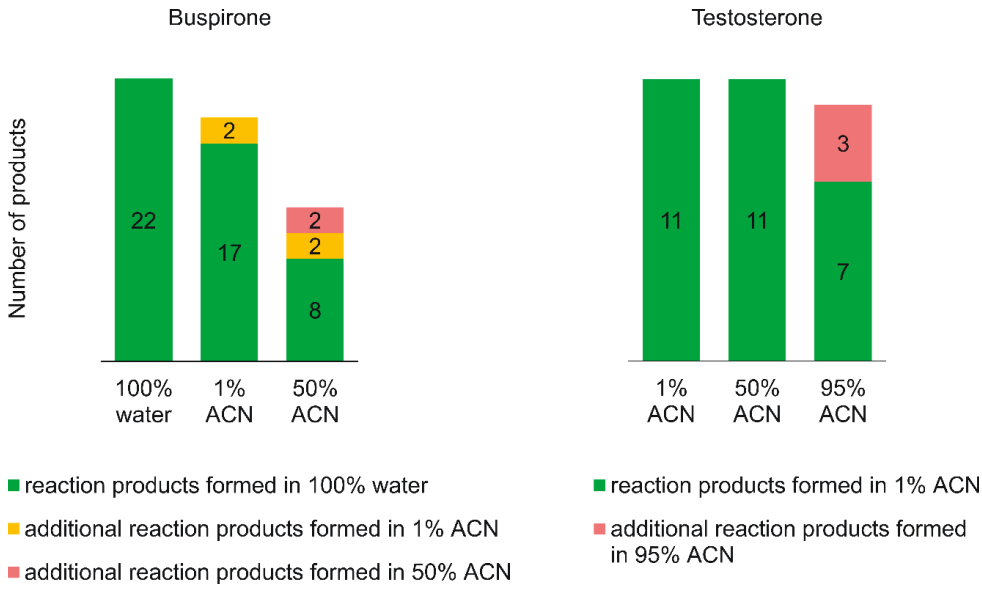

Figure 7 *Effect of acetonitrile on the TiO_2 photocatalytic reaction products of buspirone and testosterone.*

4.2.2 Comparison of titanium dioxide photocatalysis, electrochemical oxidation, and electrochemically assisted Fenton reaction for imitation of phase I metabolism

The TiO_2 photocatalytic, EC, and EC-Fenton reaction products of buspirone, promazine, testosterone, and 7-ethoxycoumarin were compared with the *in vitro* phase I HLM metabolites using UHPLC-MS (II). The high resolving power of the UHPLC allowed separation of nearly all isomeric compounds. The good repeatability of the retention times (RSD typically less than 0.5%), together with the mass spectrometric data, enabled reliable comparison of the products of different oxidation methods. All reaction products were observed as protonated molecules. In most cases, the product ion spectra of the imitation reaction products and HLM metabolites with the same *m/z* of the protonated molecule (tolerance 30 ppm) and retention time (tolerance 0.05 min) correlated well, indicating that products and metabolites identified on the basis of *m/z* and retention time were indeed the same. In the few cases where the product ion spectra were different, products having the same retention time and precursor ion probably were different isomers.

To compare the reaction product profiles of different oxidation methods, the abundances of the reaction products were normalized relative to the most abundant reaction product obtained with the particular method. Products were classified as major (S), medium (M), or

minor (W) according to their relative abundances (50–100%, 20–50% and 5–20%, respectively). In view of the many trace products, reaction products of less than 5% relative abundance were excluded from the comparison of the reaction products. Figure 8 shows the main reaction pathways of buspirone, promazine, testosterone, and 7-ethoxycoumarin. The product ion spectra allowed tentative structural assignment of most reaction products of buspirone, promazine, and 7-ethoxycoumarin. The oxidation sites of the isomeric reaction products of testosterone could not be identified based on the product ion spectra, but a major product was identified as androstenedione using a standard. The detailed comparison of the reaction products formed in HLM incubations, TiO_2 photocatalysis, EC-Fenton, and direct EC is presented in Tables 10-13, and the reactions are briefly discussed by compound.

Buspirone

The HLM metabolism reactions of buspirone included aromatic hydroxylation, aliphatic hydroxylation of R3 and R4 with or without subsequent dehydrogenation, N-oxidation of R2, loss of the ethylene group from R2, N-dealkylation between R2 and R3, and combinations of these (Table 10, see Figure 8 for explanation of the R-groups). All of these reaction types, except N-oxidation, were observed in TiO_2 photocatalysis and EC-Fenton, but the combinations of reactions and isomers were often different from those in HLM metabolism. The oxidation reactions were mostly similar in TiO_2 photocatalysis and EC-Fenton, and typically proceeded further than in HLMs; for example, dehydrogenation followed hydroxylation, and multiple hydroxylations of pyrimidine and opening or fragmentation of the pyrimidine ring were observed. EC was not capable of aromatic or aliphatic hydroxylation, but was the only imitation method that produced N-oxides, as suggested by the late elution[117] and the product ion spectra of these products.

Promazine

HLM metabolism reactions of promazine included N-demethylation, S-oxidation, aromatic hydroxylation, N-oxidation, and dehydrogenation, alone or in different combinations (Table 11, Figure 8). TiO_2 photocatalysis and EC-Fenton mainly produced sulfoxides and aromatic hydroxylation products. EC also produced sulfoxides and was the only imitation method capable of N-dealkylation of promazine. None of the imitation methods produced the HLM metabolite promazine N-oxide. Again, the oxidation typically proceeded further in TiO_2 photocatalysis and EC-Fenton than in HLM reactions.

Testosterone

The main reactions of testosterone in phase I HLM metabolism, TiO_2 photocatalysis, and EC-Fenton reactions were hydroxylation and dehydrogenation and combinations of these, but the isomers were partly different in each system (Table 12, Figure 8). Minor reactions unique to each of the systems were also observed. Direct EC failed to oxidize testosterone at all.

7-ethoxycoumarin

TiO_2 photocatalysis and EC-Fenton imitated only the main HLM metabolism reaction of 7-ethoxycoumarin, which was O-deethylation leading to 7-hydroxycoumarin (Table 13, Figure 8). Overall, the HLM, TiO_2 photocatalysis, and EC-Fenton reactions of 7-

ethoxycoumarin produced only a few products. Direct EC failed to oxidize 7-ethoxycoumarin at all.

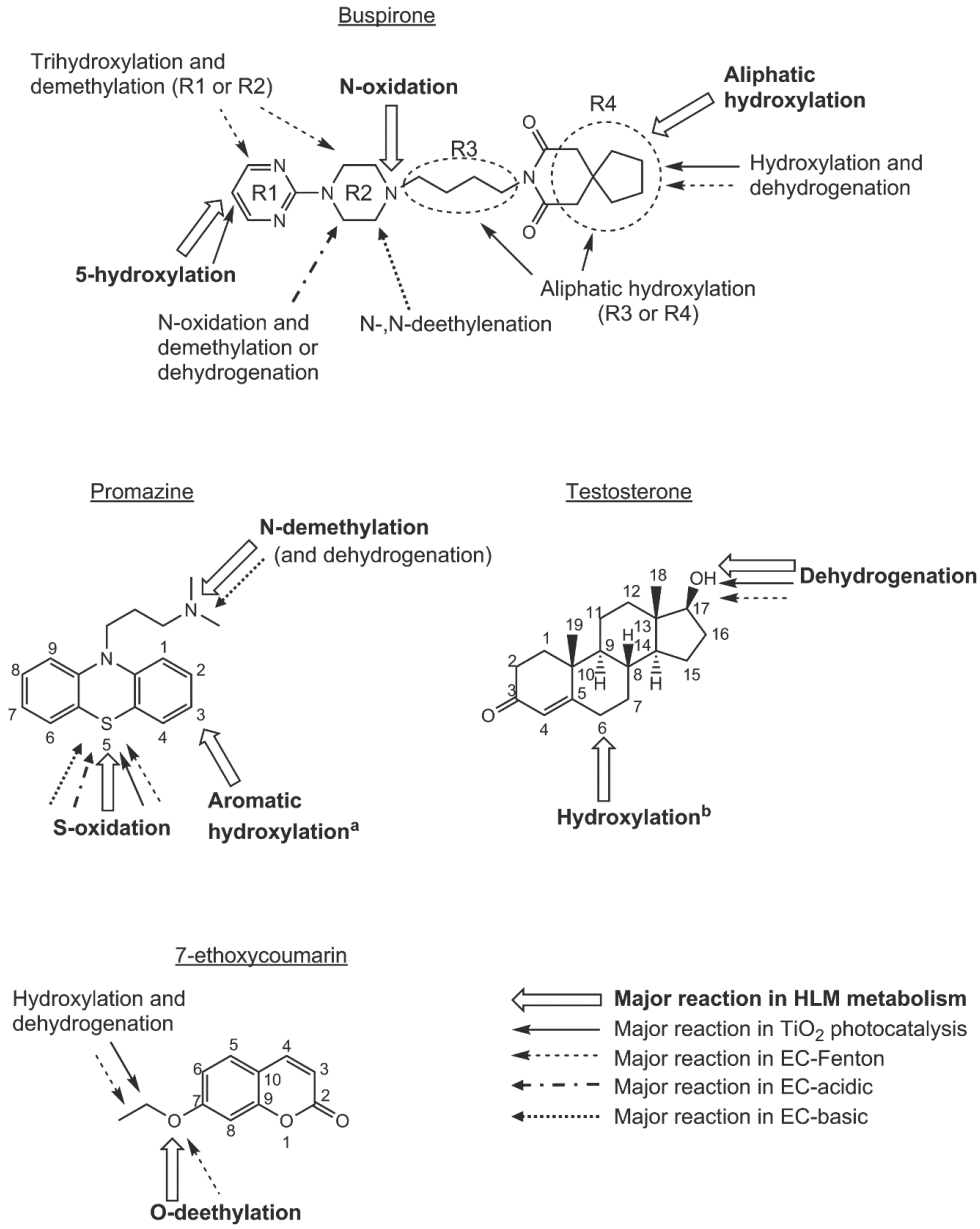

Figure 8 *Pathways for formation of the main reaction products of buspirone, promazine, testosterone, and 7-ethoxycoumarin in HLM metabolism, TiO_2 photocatalysis, EC-Fenton, and direct EC (see Table 1 for examples of the reactions).* [a] *Aromatic hydroxylation of the 3-position most likely* [136]; [b] *Allylic hydroxylation of the 6β-position most likely.* [137, 138]

Table 10. *Imitation of HLM metabolites of buspirone by TiO_2 photocatalysis, EC-Fenton, and EC.*

$[M+H]^+$ (calc.)	Reaction product	Formula	t_R (min)	Tentative structural assignment	HLM	TiO_2	EC-Fenton	EC-acidic	EC-basic
386.256	Buspirone	$C_{21}H_{31}N_5O_2$	5.03		x	x	x	x	x
402.251	M+O [a,b,c]	$C_{21}H_{31}N_5O_3$							
			2.61	Hydroxylation of R3 or R4	M	S	W		
			2.79	Hydroxylation of R4 [d]	M	W			
			3.22	Hydroxylation of R4		M	W		
			3.44	Hydroxylation of R4	M				
			4.18	Hydroxylation of R4	S	W			
			4.86	Hydroxylation of R1 [d]	S	S			
			5.59	N-oxidation of R2	S				
165.114	M-R3-R4 [a,c,d]	$C_8H_{12}N_4$	0.80	N-dealkylation	M	W	W	W	W*
240.160	M+O-R1-R2 [c]	$C_{13}H_{21}NO_3$	5.30	Hydroxylation of R3, N-dealkylation	M				
418.245	M+2O [b,c]	$C_{21}H_{31}N_5O_4$							
			2.45	Dihydroxylation of R4			W		
			2.53	Hydroxylation of R1 and R4 [d]	W	W			
			3.05	Dihydroxylation of R4		M	M		
			3.19	Hydroxylation of R4, N-oxidation of R2	W				
			3.50	Dihydroxylation of R4		W	M		
			3.96	Dihydroxylation of R4	W				
			4.02	Hydroxylation of R1 and R3 or R4	M				
			4.79	Hydroxylation of R4, N-oxidation of R2	W				
			5.38	Hydroxylation of R2 and R4			W		
			5.50	Hydroxylation of R4, N-oxidation of R2	W				

Table 10 continued *Imitation of HLM metabolites of buspirone by TiO_2 photocatalysis, EC-Fenton and EC.*

$[M+H]^+$ (calc.)	Reaction product	Formula	t_R (min)	Tentative structural assignment	HLM	TiO_2	EC-Fenton	EC-acidic	EC-basic
254.139	M+2O-2H-R1-R2 [c]	$C_{13}H_{19}NO_4$	4.92	Dihydroxylation and dehydrogenation of R3, N-dealkylation	W				
360.240	M-C_2H_2 [b]	$C_{19}H_{29}N_5O_2$	4.38	N,N-deethylenation of R2	W	M	M	M	S
400.235	M+O-2H	$C_{21}H_{29}N_5O_3$							
			2.24	Hydroxylation and dehydrogenation of R4 [d]	W	S	S		
			2.83	Hydroxylation and dehydrogenation of R4		S	M		
			5.40	Hydroxylation and dehydrogenation of R2			W		
			5.53	Hydroxylation and dehydrogenation of R3 or R4		W	W		
			6.06	Hydroxylation and dehydrogenation of R2		W	W		
384.240	M-2H [b]	$C_{21}H_{29}N_5O_2$							
			4.69	Dehydrogenation of R2	W	M	W		
			5.38	Dehydrogenation of R2		W	M		
			5.55	Dehydrogenation of R2		W	W		
235.145	M-151	$C_{13}H_{18}N_2O_2$	5.26	N,N-dealkylation of R2, 2x dehydrogenation					W
308.234	M-R1 [c,d]	$C_{17}H_{29}N_3O_2$	3.59	N-dealkylation		W	M		
350.256	M-36 [d]	$C_{18}H_{31}N_5O_2$	3.05	Fragmentation of R1		W	M		
372.240	M-CH_2	$C_{20}H_{29}N_5O_2$	4.43	Demethylation				M	S
378.251	M-8	$C_{19}H_{31}N_5O_3$	3.32	Hydroxylation and fragmentation of R1		M	M		
388.235	M+O-CH_2	$C_{20}H_{29}N_5O_3$							
			4.33	Hydroxylation and demethylation of R2		W	W		
			6.76	N-oxidation and demethylation of R2				S	M
398.219	M+O-4H	$C_{21}H_{27}N_5O_3$	2.46	Hydroxylation and 2x dehydrogenation		W			
406.245	M+20	$C_{20}H_{31}N_5O_4$	3.49	Dihydroxylation and fragmentation of R1		M			

Table 10 continued *Imitation of HLM metabolites of buspirone by TiO_2 photocatalysis, EC-Fenton, and EC.*

$[M+H]^+$ (calc.)	Reaction product	Formula	t_R (min)	Tentative structural assignment	HLM	TiO_2	EC-Fenton	EC-acidic	EC-basic
408.261	M+2O	$C_{20}H_{33}N_5O_4$	3.32	Dihydroxylation and fragmentation of R1			W		
414.214	M+2O-4H	$C_{21}H_{27}N_5O_4$	5.50	Dihydroxylation 2x dehydrogenation of R2			W		
415.246	M+O+NH_3-2H	$C_{21}H_{31}N_6O_3$	5.10	Hydroxylation and dehydrogenation of R2, addition of ammonia to R2					M
416.230	M+2O-2H	$C_{21}H_{29}N_5O_4$							
			2.16	Hydroxylation of R2, hydroxylation and dehydrogenation of R4		W			
			2.73	Hydroxylation of R1, hydroxylation and dehydrogenation of R4		W			
			7.13	2x N-oxidation and dehydrogenation of R2				S	W
420.225	M+3O-CH_2	$C_{20}H_{29}N_5O_5$	7.24	Trihydroxylation and demethylation of R1 or R2			S		
434.204	M+4O-CH_2	$C_{20}H_{27}N_5O_6$	4.05	Trihydroxylation and demethylation of R1, hydroxylation and dehydrogenation of R4			W		
434.240	M+3O [c]	$C_{21}H_{31}N_5O_5$	2.56	Trihydroxylation of R4		W	W		
438.272	M+3O+4H	$C_{21}H_{35}N_5O_5$							
			2.65	Trihydroxylation of R1, opening of pyrimidine ring, 2 x hydrogenation		M	W		
			2.75	Trihydroxylation of R1, opening of pyrimidine ring, 2 x hydrogenation		W	W		

S = 50–100%, M = 20–50%, W = 5–20% of the peak area of the most abundant reaction product of the particular method.
Buspirone groups R1-R4 are explained in Figure 8.
Observed earlier in HLM incubations: [a] five M+O metabolites: 5-hydroxybuspirone, 3'-hydroxybuspirone, 6'-hydroxybuspirone, oxa-buspirone and buspirone N-oxide [139]; [b] six M+O metabolites, seven M+2O metabolites [140]; [c] six M+O metabolites, seven M+2O metabolites, three M+O metabolites.[141]
[d] Observed earlier in TiO_2 photocatalysis: hydroxylation of R4: three M+O products; hydroxylation and dehydrogenation of R4: two M+O-2H products; hydroxylation of both R1 and R4: two M+2O products.[30]
* Produced at 800 mV. Other EC-acidic and EC-basic reaction products were produced at 1000 mV and 1200 mV potentials, respectively.

Table 11. *Imitation of HLM metabolites of promazine by TiO_2 photocatalysis, EC-Fenton, and EC.*

$[M+H]^+$ (calc.)	Reaction product	Formula	t_R (min)	Tentative structural assignment	HLM	TiO_2	EC-Fenton	EC-acidic	EC-basic
285.143	Promazine	$C_{17}H_{20}N_2S$	6.95		x	x			x
271.127	M-CH_2	$C_{16}H_{18}N_2S$	7.05	N-demethylation [a]	S				S
301.138	M+O	$C_{17}H_{20}N_2OS$							
			3.97	S-oxidation [a,b]	S	S	S	S	M
			5.57	Aromatic hydroxylation	S	W			
			7.71	N-oxidation	M				
287.122	M+O-CH_2	$C_{16}H_{18}N_2OS$							
			3.95	S-oxidation, N-demethylation	W			W	S
			5.64	Aromatic hydroxylation, N-demethylation	W				
317.132	M+2O [b]	$C_{17}H_{20}N_2O_2S$							
			3.36	M+2O in phenothiazine		W			
			3.62	S-oxidation, hydroxylation of phenothiazine	W	M	W		
			4.05	M+2O in phenothiazine		W			
			4.30	2x S-oxidation			W	M*	
			4.45	S-oxidation and N-oxidation or aliphatic hydroxylation	W	W			
			4.61	M+2O in phenothiazine		W			
315.117	M+2O-2H	$C_{17}H_{18}N_2O_2S$							
			4.71	S-oxidation, aromatic hydroxylation, dehydrogenation		W			
			5.84	S-oxidation, N-oxidation, dehydrogenation	W			W	
319.148	M+2O+2H	$C_{17}H_{22}N_2O_2S$	4.90			W			
333.127	M+3O	$C_{17}H_{20}N_2O_3S$	4.81	2x S-oxidation, aromatic hydroxylation		W	W		
335.143	M+3O+2H	$C_{17}H_{22}N_2O_3S$	5.17	2x S-oxidation, aromatic hydroxylation, hydrogenation		W			

Table 11 continued *Imitation of HLM metabolites of promazine by TiO_2 photocatalysis, EC-Fenton, and EC.*

$[M+H]^+$ (calc.)	Reaction product	Formula	t_R (min)	Tentative structural assignment	HLM	TiO_2	EC-Fenton	EC-acidic	EC-basic
216.048	M+O-$C_5H_{11}N$	$C_{12}H_9NSO$	5.82	phenothiazine sulfoxide (resulting from S-oxidation, N-dealkylation)					M
269.111	M-CH_4	$C_{16}H_{16}N_2S$	2.95	N-demethylation, dehydrogenation					S
273.106	M+O-2CH_2	$C_{15}H_{16}N_2OS$	3.93	S-oxidation, 2x N-demethylation				W	W
299.122	M+O-2H	$C_{17}H_{18}N_2OS$	1.29	S-oxidation, dehydrogenation				W	W*
300.117	M+O+NH_3-CH_2-4H	$C_{16}H_{17}N_3OS$	4.86	S-oxidation, N-demethylation, 2x dehydrogenation, addition of ammonia					M
302.133	M+O+NH_3-CH_2-2H	$C_{16}H_{19}N_3OS$	2.86	S-oxidation, N-demethylation, dehydrogenation, addition of ammonia					M*

S = 50–100%, M = 20–50%, W = 5–20% of the peak area of the most abundant reaction product of the particular method.
EC-acidic and EC-basic reaction products were produced at 1000 mV and 600 mV potentials, respectively.
[a] Observed earlier in HLM incubations.[136]
[b] Observed earlier in EC experiments: two M+2O products.[142]

Table 12. *Imitation of HLM metabolites of testosterone by TiO_2 photocatalysis, EC-Fenton, and EC.*

$[M+H]^+$ (calc.)	Reaction product	Formula	t_R (min)	HLM	TiO_2	EC-Fenton
289.217	Testosterone	$C_{19}H_{28}O_2$	9.44	x	x	x
305.212	M+O [a, b]	$C_{19}H_{28}O_3$				
			3.41			W
			4.25	M	W	W
			4.54		W	W
			4.82			W
			5.35	S		W
			5.87	M	W	M
			6.34		W	W
			6.72	W	W*	W*
			6.94	W		
			6.99		W	W
			7.20	W	W	W
			7.50	M		
287.201	M-2H [a, c]	$C_{19}H_{26}O_2$				
			8.72	S	S	S
			9.13		W	M*
			9.25	W	W	M*
303.196	M+O-2H	$C_{19}H_{26}O_3$				
			4.14	W		
			4.55		M	W
			4.97		W	
			5.12	W		
			5.32			W
			5.40	W	M	W
			6.01		W	W
			6.42		W	W
			7.29	W		
285.186	M-4H	$C_{19}H_{24}O_2$	8.26	W		
301.180	M+O-4H	$C_{19}H_{24}O_3$	2.37		W	
323.186	M+3O-CH_2	$C_{18}H_{26}O_5$	9.96			M

S = 50–100%, M = 20–50%, W = 5–20% of the peak area of the most abundant reaction product of the particular method.

[a] Observed earlier in HLM incubations: androstenedione, 1α-, 1β-, 2α-, 2β-, 6α-, 6β-, 7α-, 11β-, 15β-, 16α-, 16β-, and 18/12α-hydroxylation, 6β the major hydroxylation site (see Figure 8) [137, 138, 143, 144];

[b] Observed earlier in EC-Fenton experiments: two M+O products [26];

[c] The major M-2H product was androstenedione, as confirmed through comparison with a standard by MS/MS.

* The product ion spectrum does not correlate well enough with the spectrum of the HLM metabolite, indicating different isomers.

Table 13. *Imitation of HLM metabolites of 7-ethoxycoumarin by TiO_2 photocatalysis, EC-Fenton, and EC.*

$[M+H]^+$ (calc.)	Reaction product	Formula	t_R (min)	Tentative structural assignment	HLM	TiO_2	EC-Fenton
191.071	7-ethoxy-coumarin	$C_{11}H_{10}O_3$	6.64		x	x	x
163.040	M-C_2H_4 [a]	$C_9H_6O_3$	3.79	Deethylation to 7-hydroxycoumarin	S	M	S
183.102	M+O+4H-CO	$C_{10}H_{14}O_3$	4.64		M		
179.034	M+O-C_2H_4	$C_9H_6O_4$	2.73	Hydroxylated 7-hydroxycoumarin [b]	W		
197.081	M+O-CH_2+4H	$C_{10}H_{12}O_4$	3.92		W		
205.050	M+O-2H	$C_{11}H_8O_4$	4.32	Hydroxylation and dehydrogenation of the ethylene moiety		S	S
207.066	M+O [a]	$C_{11}H_{10}O_4$					
			4.69	Hydroxylation of			M
			4.78	coumarin		M	W

S = 50–100%, M = 20–50%, W = 5–20% of the peak area of the most abundant reaction product of the particular method.
[a] Observed earlier in HLM incubations: 7-hydroxycoumarin, 3- and 6-hydroxylations [143]; [b] 3-hydroxylation (see Figure 8 for numbering) is most likely to occur.[145, 146]

TiO_2 photocatalysis was able to produce almost half (44%) of the HLM metabolites; the coverage was considerably poorer for EC-Fenton (31%), and direct EC (coverage 11%) failed to produce most of the HLM metabolites (Equation 2). All of the imitation methods produced also several products other than HLM metabolites (Figure 9). In total, EC produced the smallest number of reaction products, whereas TiO_2 photocatalysis, EC-Fenton, and HLM reactions were close to each other in the total number of reaction products.

The main phase I HLM metabolism reactions of the model drugs covered the most common phase I reactions such as hydroxylation, dehydrogenation, N-dealkylation, O-dealkylation, N-oxidation, and S-oxidation (Table 14). All of these reaction types, except N-oxidation, were observed commonly in TiO_2 photocatalysis and EC-Fenton reactions, where the hydroxyl radical-based mechanism enables reactions beginning with hydrogen atom abstraction. However, TiO_2 photocatalysis and EC-Fenton reaction often overoxidized the compounds (e.g. hydroxylation followed by dehydrogenation) as compared with *in vitro* metabolism. Direct EC was mainly capable of N-dealkylation and S-oxidation reactions, which can begin with single electron transfer. TiO_2 photocatalytic reaction can begin both by hydrogen atom abstraction by hydroxyl radicals and by single electron transfer to an electron hole on the TiO_2 surface, both of which are essential mechanisms in CYP450 catalyzed phase I metabolism. This may account for the better ability of TiO_2 photocatalysis to imitate HLM metabolites relative to EC and EC-Fenton. TiO_2 photocatalysis was also much faster than EC-Fenton and the traditional *in vitro* methods. Despite the possibility for the same reaction types, different isomeric products and combinations of reactions often

occurred, owing to the different selectivities of the compared oxidation methods. All in all, the highly selective enzymatic reactions cannot be comprehensively imitated by any of the imitation methods and none of the compared imitation methods allow exact prediction of the metabolism of a novel drug. Nonetheless, some of the imitation reaction products not found in HLM could be clinically relevant, as all of the drug-metabolizing enzymes are not present in HLMs. In addition, other nonbiological oxidation products could form through, for example, incorrect storage of the medicinal preparation.

(2) $$Coverage = \frac{number\ of\ the\ same\ reaction\ products\ in\ imitation\ reactions\ and\ HLM\ reactions}{total\ number\ of\ metabolites\ produced\ by\ HLM}\ x\ 100\%$$

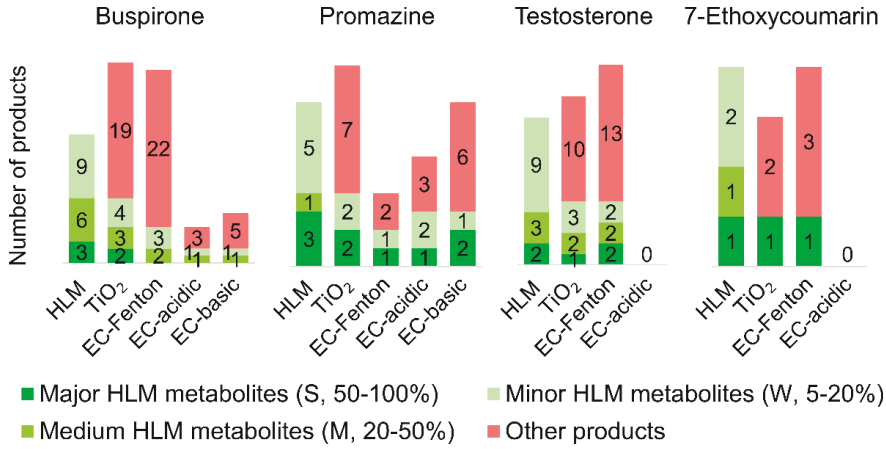

Figure 9 *Summary of imitation of HLM metabolites of buspirone, promazine, testosterone, and 7-ethoxycoumarin by TiO_2 photocatalysis, EC-Fenton, and EC. The number of the products is given in the bars. No reaction products of testosterone and 7-ethoxycoumarin were observed in EC-acidic.*

Table 14. *Main reaction types observed in HLM phase I metabolism, TiO_2 photocatalysis, EC-Fenton, and EC reactions.*

	Aliphatic hydroxylation	Aromatic hydroxylation	Dehydro-genation	N-oxidation	S-oxidation	N-dealkylation	O-dealkylation	Hydro-genation	Addition of ammonia
Buspirone									
HLM	x	x	x	x	n.a.	x	n.a.		
TiO_2	x	x	x		n.a.	x	n.a.	x	
EC-Fenton	x	x	x		n.a.	x	n.a.	x	
EC-acidic			x	x	n.a.	x	n.a.		
EC-basic			x	x	n.a.	x	n.a.		x
Promazine									
HLM		x	x	x	x	x	n.a.		
TiO_2		x	x		x		n.a.		
EC-Fenton		x			x		n.a.		
EC-acidic			x		x	x	n.a.		
EC-basic			x		x	x	n.a.		x
Testosterone									
HLM	x	n.a.	x	n.a.	n.a.	n.a.	n.a.		
TiO_2	x	n.a.	x	n.a.	n.a.	n.a.	n.a.		
EC-Fenton	x	n.a.	x	n.a.	n.a.	n.a.	n.a.		
EC-acidic		n.a.		n.a.	n.a.	n.a.	n.a.		
7-ethoxycoumarin		hydroxylation of the coumarin structure							
HLM		x		n.a.	n.a.	n.a.	x	x	
TiO_2	x	x	x	n.a.	n.a.	n.a.	x		
EC-Fenton	x	x	x	n.a.	n.a.	n.a.	x		
EC-acidic				n.a.	n.a.	n.a.			

n.a. = reaction not applicable for the compound

4.2.3 Imitation of phase I metabolism of anabolic steroids by titanium dioxide photocatalysis

Compared with EC and EC-Fenton, TiO_2 photocatalysis proved the most suitable for oxidation of nonpolar compounds such as testosterone (II). Thus, TiO_2 photocatalysis was also applied to imitation of phase I metabolism of anabolic steroids (III). The photocatalytic reaction products of commonly used doping substances metandienone, methyltestosterone, nandrolone, stanozolol, and testosterone were compared with their phase I metabolites produced by HLMs.

The good chromatographic performance of the developed UHPLC-MS method was recognized as narrow, and non-tailing peaks, and relative standard deviations of retention times were typically less than 0.25%. This allowed separation of several isomeric oxidation products formed in HLM metabolism and TiO_2 photocatalysis. ESI mass spectra of the anabolic steroids and their oxidation products showed an abundant protonated molecule with few fragment ions typically formed by the loss of one or two water molecules. A few products observed with the same *m/z* and retention time in the HLM metabolism and TiO_2 photocatalysis showed, however, differing product ion spectra, indicating that these products were different isomers. The different isomeric products can be attributed to the different selectivity of the enzymatic reactions and the hydroxyl radical attack in TiO_2 photocatalysis.

The main reaction types both in TiO_2 photocatalysis and phase I HLM metabolism of the anabolic steroids were hydroxylation (M+O), dehydrogenation (M-2H), and a combination of these (M+O-2H) (Figure 10, see Table 1 for examples of the reactions). In total, TiO_2 photocatalysis produced 31% of all the HLM reaction products of all the steroids studied (Equation 2). The HLM metabolites and photocatalytic reaction products of testosterone conformed well to those found in Study II. As a whole, the main phase I HLM metabolism reactions of methyltestosterone, nandrolone, testosterone, and stanozolol were imitated considerably better than those of metandienone. The reaction products are briefly discussed by product type below.

TiO_2 photocatalysis produced 50% of the M-2H metabolites of the anabolic steroids studied (Equation 2). The M-2H metabolites of structurally similar methyltestosterone, nandrolone, and testosterone were imitated well by TiO_2 photocatalysis (Figure 10). The main M-2H product of testosterone was identified as androstenedione by comparison of the product ion spectrum to that of a standard. 17-keto metabolites are the main excreted metabolites of anabolic steroids having a secondary 17β-hydroxy group such as testosterone and nandrolone (see testosterone in Figure 10 for numbering of the steroid skeleton).[147] Thus, the main M-2H product of nandrolone is most likely formed by oxidation of 17β-hydroxyl to ketone. Metandienone, methyltestosterone, and stanozolol also formed an M-2H metabolite each. Nevertheless, the 17α-methyl group of methyltestosterone, metandienone, and stanozolol should inhibit their 17β-oxidation. Therefore, the M-2H metabolite is likely to result from formation of a double bond in the steroid skeleton. The most obvious site of dehydrogenation in the steroid skeleton is the C6-C7 bond since in this case the increased degree of conjugation of double bonds stabilizes the product *via* π-

electron delocalization. Dehydrogenation of the C6-C7 bond has also been observed in human *in vivo* metabolism of methyltestosterone[148] and metandienone.[147] A few isomeric M-2H products, which were not formed in HLM reactions, were formed in TiO_2 photocatalysis of each of the steroids.

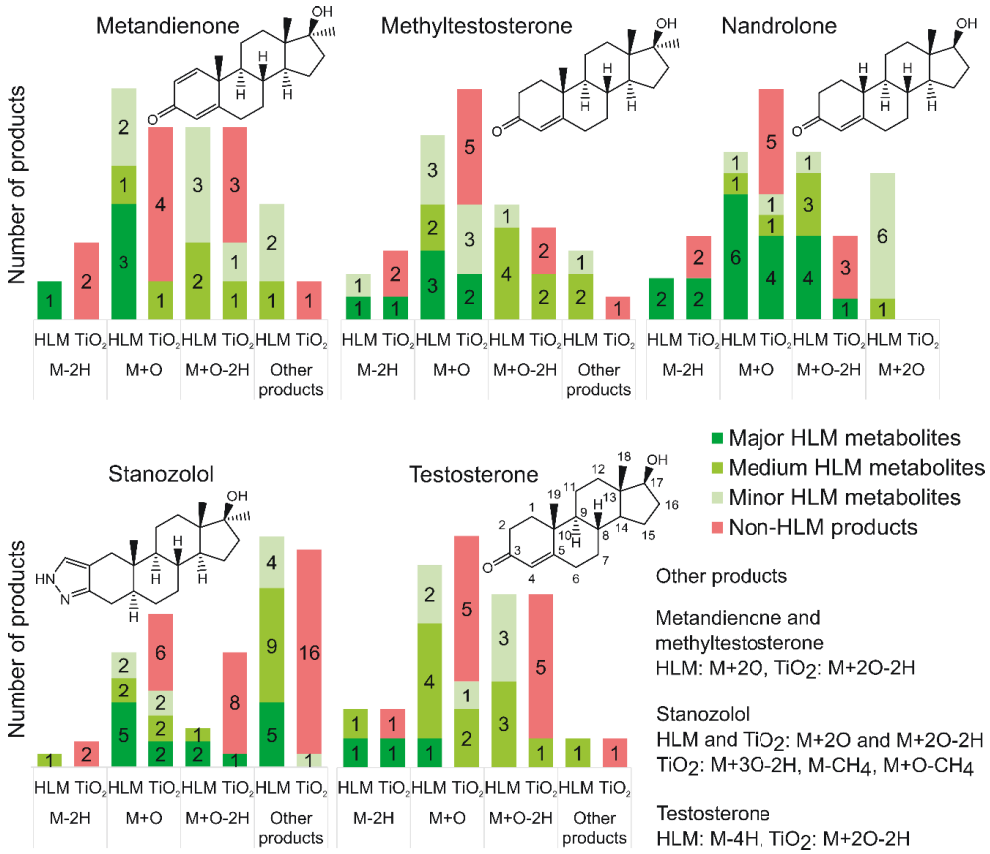

Figure 10 *Imitation of steroid HLM metabolites by TiO_2 photocatalysis.The number of the products is given in the bars.*

TiO_2 photocatalysis imitated 55% the M+O metabolites of all the steroids studied (Equation 2). The M+O metabolites of metandienone were imitated remarkably poorer than those of other steroids (Figure 10). Seven hydroxylation products were observed in HLM metabolism of testosterone. These include most likely the 1β-, 2β-, 6β-, 11β-, 15β-, and 16β-hydroxytestosterones previously found in HLM reactions, of which the 6β-hydroxylation product is the dominant metabolite.[137, 138, 144] Also minor 1α-, 2α-, 6α-, 7α-, 16α-, and 18/12α-hydroxylation products of testosterone have been found in HLM incubations.[143] The metabolism of the other steroids used in this study has mainly been examined using human subjects,[149-151] various animal species,[152-154] or *in vitro* using liver preparations from different animals.[143, 155] These former studies cannot, however, be directly compared

with the HLM results in this work because of species differences in metabolism and differences between excreted metabolites and other metabolites formed in the body.

Generally, TiO_2 photocatalysis imitated the M+O-2H metabolites poorer (26%) than the M-2H and the M+O metabolites (Figure 10). The combination of two reactions can produce more possible isomers and the probability that the same isomers are formed in both systems is lower. In addition to M-2H, M+O, and M+O-2H products, dihydroxylation products (M+2O) were formed mainly in HLM reactions, and products formed by dihydroxylation+dehydrogenation (M+2O-2H) were favored by TiO_2 photocatalytic reactions. This implies that the oxidation proceeds further in TiO_2 photocatalysis than in HLM metabolism, as also observed in Study II. In addition, a few other minor oxidation products were observed in TiO_2 photocatalysis (Figure 10).

Importantly, TiO_2 photocatalysis proved capable of producing over half of the M+O products of anabolic steroids. Capability of aliphatic hydroxylation is essential for the imitation of phase I metabolism of anabolic steroids, which can be enzymatically hydroxylated at numerous sites.[138, 141, 149, 150, 156, 157] TiO_2 photocatalysis may provide a valuable way to oxidize also other nonpolar and hydrophobic compounds.

4.3 Titanium dioxide photocatalysis – desorption electrospray ionization mass spectrometry rotating array platform

TiO_2 photocatalytic reactions are very fast, especially if no organic solvent is needed. However, the removal of the nanoparticles and the LC-MS analysis step are time-consuming. A TiO_2-coated nanoreactor μPESI chip provided much faster photocatalytic experiments than conventional methods.[31] The fabrication of μPESI chip is, however, demanding and requires the use of expensive clean-room facilities. To omit the complicated microfabrication and the need for pretreatment and to enhance the speed of analysis, a TiO_2 photocatalysis-DESI-MS rotating array platform for high-throughput screening of oxidation products was developed in this study. For this purpose, a round glass wafer was coated with photocatalytically active anatase-phase TiO_2 using atomic layer deposition. The same TiO_2-coated glass wafer was used as a sample platform for photocatalytic reactions and DESI-MS analysis (Figure 11). The performance of the TiO_2 photocatalysis-DESI-MS rotating array platform was characterized and its capability for imitation of phase I metabolism reactions was studied using amodiaquine, buspirone, and verapamil as model drug compounds. The feasibility of the platform for high-throughput screening of oxidation products was investigated using 12 model drug compounds (amodiaquine, buspirone, verapamil, amphetamine, propranolol, metoprolol, nicotine, lidocaine, quinidine, moperone, atenolol, and nadolol).

The X-ray diffraction analysis of the TiO_2-coated glass wafer proved that the film crystal structure was photoactive polycrystalline anatase, which provides efficient and fast TiO_2 photocatalytic oxidation reactions.[31, 95-97] Microscopic examination of the coated wafer appearance and the UV-VIS reflectometry showed the TiO_2 film was uniform, with a thickness of 100 nm ensuring repeatable oxidation experiments. Owing to the stability of

the film, the TiO_2-coated glass wafer could be reused by washing the sample residues from the surface after DESI analysis.

The volume of the sample needed for the oxidation reaction was only 1 µL. This is significantly less than in nanoparticle-based photocatalytic methods or in *in vitro* metabolism assays, where the sample volumes are typically hundreds of microliters. Approximately 70 samples could be introduced onto the rim of one TiO_2-coated glass wafer (Figure 11), allowing high-throughput experiments.

All samples on the TiO_2-coated glass wafer could be exposed to UV at the same time offline using large diameter UV lamp (Figure 11a). UV exposure times of 30 s, 45 s, and 120 s were the most suitable for producing oxidation products of verapamil, buspirone, and amodiaquine, respectively. Longer exposure times resulted in increased decomposition. Analysis of samples from an uncoated glass wafer with UV exposure as well as from TiO_2-coated glass without UV exposure showed no oxidation products. Thus, the oxidation products of the model compounds were formed only upon UV-initiated TiO_2 photocatalytic oxidation reactions.

Alternatively, the samples were UV exposed online while the TiO_2-coated glass wafer rotated and transferred the exposed samples to DESI-MS analysis (Figure 11b). The reaction products of amodiaquine, buspirone, and verapamil obtained using online (100-120 s) UV exposure were similar to those obtained *via* offline exposure. In the online method, the exposure time was determined by the diameter of the UV beam and the rotation speed, which must be optimized to allow proper exposure and analysis times. Therefore, the offline mode offered higher throughput than the online mode in this work.

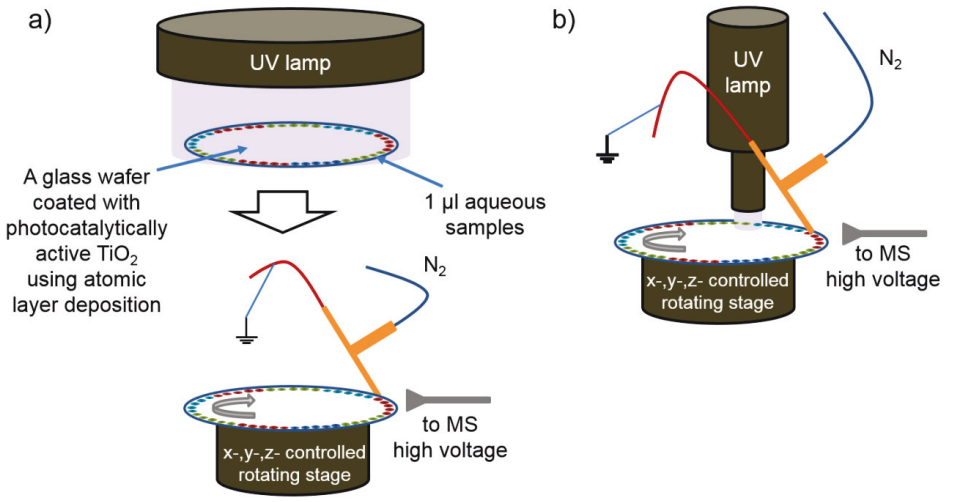

Figure 11 *A schematic picture of the experimental a) offline and b) online TiO_2 photocatalysis–DESI-MS rotating array platform setups (not in scale). MS = mass spectrometer.*

The repeatability and sensitivity of DESI-MS analysis were dependent on the rotation speed of the wafer and positioning of the DESI sprayer and sample relative to the capillary extension inlet. In this work, the optimal rotation speed for maximum sensitivity and stability was 15 mm min^{-1}, which allowed analysis of four samples within one minute. As previously reported,[158] the positioning of the DESI sprayer and the sample spot relative to the flared capillary extension inlet was not as critical as with a conventional "straight" capillary extension inlet. The signal-to-noise ratio was highest when the distance of the sample from the flared capillary extension inlet was between 10 mm and 17 mm and did not significantly change within this range. The repeatability of the method was tested with verapamil samples exposed to UV offline for 30 s (Figure 12). The average relative standard deviation of the peak areas of a six-replicate DESI-MS analysis of verapamil and its main oxidation products was 16%. The repeatability was typical for DESI-MS analysis,[159-161] although it also included the repeatability of TiO_2 photocatalysis.

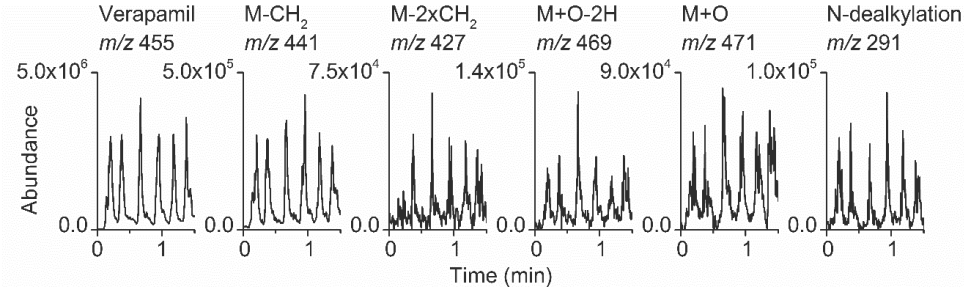

Figure 12 *Extracted ion profiles of verapamil (six parallel samples) and its main reaction products after offline TiO_2 photocatalysis of 30 s.*

To demonstrate the feasibility of the TiO_2 photocatalysis–DESI-MS rotating array platform for high-throughput screening of oxidation products, 12 drug compounds were UV exposed offline for 30 s. Oxidation products of all test compounds were observed using only one compromised UV exposure time (Table 15). However, optimization of the UV exposure time separately for each compound might enable more efficient conversion of the compounds to the products.

The feasibility of the TiO_2 photocatalysis–DESI-MS rotating array platform for imitation of drug metabolism reactions was studied with buspirone, verapamil, and amodiaquine as model drug compounds. The DESI-MS spectra of the model compounds and their oxidation products showed abundant protonated molecules ($[M+H]^+$), which were used as precursor ions in MS/MS analysis. The main TiO_2 photocatalytic oxidation products detected were formed by oxidation, hydroxylation, demethylation, and dehydrogenation and their various combinations (Table 16). The photocatalytic reaction products of buspirone and verapamil conformed well to the product types observed earlier in TiO_2 photocatalysis and HLM metabolism (II).[30, 31] However, in the case of amodiaquine, only a minor hydroxylation product was observed. Aromatic hydroxylation of amodiaquine has been reported to occur in human *in vivo* metabolism[162, 163] as well as with recombinant

cytochrome P450 enzymes[164], but in combination with other reactions such as deethylation. Aromatic hydroxylation is catalyzed by CYP1A1 and CYP1B1 isoforms, which are mainly found in extrahepatic tissues, and therefore, the reaction is not observed in HLM incubations.[164] Nevertheless, the major metabolite of amodiaquine is deethylamodiaquine.[162, 163, 165] Detection of the reactive quinone imine metabolites of amodiaquine and deethylamodiaquine[166] would likely require conjugation with, for example, glutathione, imitating phase II metabolism. Imitation of phase II conjugative metabolism in combination with TiO_2 photocatalysis was recently demonstrated by conjugating the reactive quinone imine formed in TiO_2 photocatalytic oxidation of paracetamol.[46] Minor TiO_2 photocatalytic oxidation of amodiaquine relative to verapamil and buspirone may relate to amodiaquine solution containing 0.25% acetonitrile (the stock solution was made in acetonitrile), as even 1% acetonitrile inhibited considerably the photocatalytic reaction performed with TiO_2 particles (II).

Table 15. *TiO_2 photocatalytic reaction products observed in high-throughput screening of oxidation products after 30 s offline UV exposure.*

Compound	Reaction product	$[M+H]^+$	Compound	Reaction product	$[M+H]^+$
Amodiaquine		356	**Propranolol**		260
	M+O	372		M+2O	292
Buspirone		386	**Metoprolol**		268
	M+O	402		M+O-2H	282
	M+O-2H	400	**Nicotine**		163
	M+O-CH_2	388		M+O	179
	M-C_2H_2	360	**Lidocaine**		235
	M+2O	418		M+O-2H	249
	M+2O-2H	416		M+O	251
	M-2H	384	**Quinidine**		325
	M-16	370		M-2H	323
	M-36	350		M+2O	357
Verapamil		455		M+O	341
	M-CH_2	441	**Moperone**		356
	M+O	471		M-HF	336
	N-dealkylation	291		M+O	372
	M+O-2H	469	**Atenolol**		267
	M-2xCH_2	427		M+O	283
	M+2O	487	**Nadolol**		310
Amphetamine		136		M-2H	308
	M+O	152		M+O	326
	M+O-2H	150		M+O-2H	324
	M+2O	168			

Table 16. *Reaction product types of buspirone, verapamil, and amodiaquine observed in TiO_2 photocatalysis–DESI-MS experiments, HLM metabolism[31, 167] (II), and TiO_2 photocatalysis using nanoparticles (buspirone) or µPESI chip[31] (verapamil).*

	Reaction products observed in TiO_2 photocatalysis–DESI-MS	$[M+H]^+$	Observed earlier in HLM metabolism	Observed earlier in TiO_2 photocatalysis
Buspirone		386		**Particle-based**
Main products	M+O*	402	x	x
	M+O-2H*	400	x	x
	M+O-CH_2	388		x
Minor products	M+2O	418	x	x
	M+2O-2H	416		x
	M-C_2H_2	360	x	x
	M-2H	384	x	x
Verapamil		455		**µPESI**
Main products	M-CH_2* (≥ 2 isomers)	441	x	x
	M-2xCH_2* (≥ 2 isomers)	427	x	
	M+O	471	x	x
	M+O-2H* (≥ 3 isomers)	469	x	x
	M-164, N-dealkylation	291	x	x
Minor products	M+2O	487	x	
	M+2O-CH_2	473		
Amodiaquine		356	**	No data found
	M+O*	372		

*Tentative structural assignment based on product ion spectra (Figure 13)
** See the text above for the discussion of amodiaquine metabolism.

Although DESI-MS does not allow separation of isomeric reaction products, the MS/MS analysis provides information of the modification site. The time-consuming LC-MS/MS analysis does not necessarily allow more precise determination of the modification site even if the reaction products are chromatographically separated. The product ion spectra of the main photocatalytic products in TiO_2 photocatalysis-DESI-MS rotating array platform experiment allowed identification of oxidation sites of several reaction products (Figure 13). The interpretation of the product ion spectra can be found in Manuscript IV. In the case of buspirone, the oxidation sites of the reaction products could be identified using DESI-MS/MS with similar precision as in LC-MS/MS analysis (II). However, the LC-MS/MS analysis allowed separation of several isomeric reaction products of buspirone, which were not observed based on the DESI-MS/MS spectra. In contrast, the DESI-MS/MS analysis of the M-CH_2, M-2xCH_2 and M+O-2H reaction products of verapamil allowed identification of several isomers. Nevertheless, TiO_2 photocatalysis often produces different isomers than those produced by enzymes, and analysis of these isomers may require proper chromatographic separation to avoid false matches. Furthermore, the chromatographic separation of isomeric compounds provides a more exact number of the formed reaction products, facilitates the interpretation of the MS/MS spectra of the individual separated

compounds, and allows use of data-dependent MS/MS methods as well as spectral interpretation and metabolite identification software. The DESI-MS/MS and LC-MS/MS approaches, however, are complementary and can be utilized according to the requirements of the study. The TiO_2 photocatalysis–DESI-MS rotating array platform is most suitable to applications where rapid and easy screening is needed instead of rigorous separation of possible isomeric products.

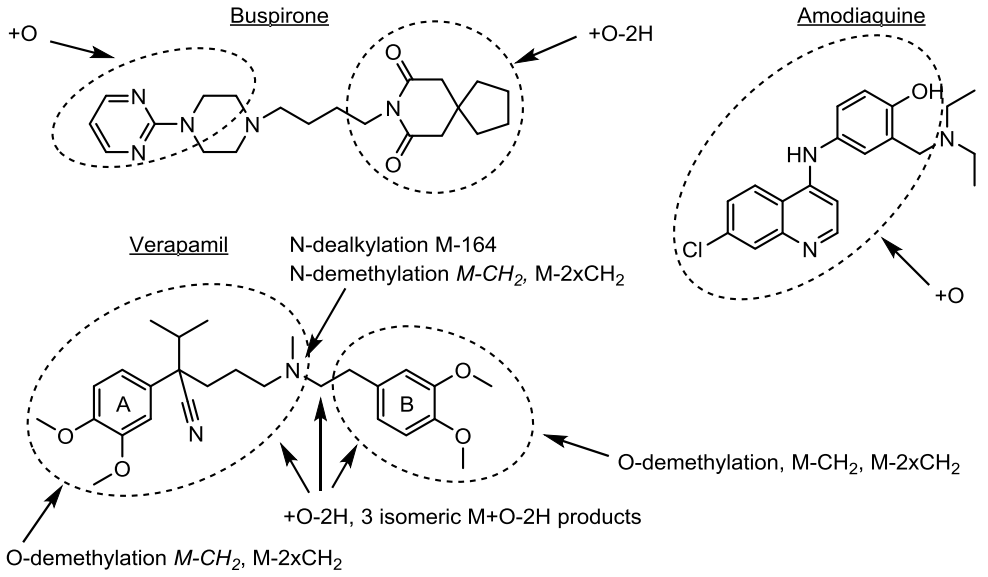

Figure 13 *Tentative structural assignment of the photocatalytic reaction products of buspirone (M+O and M+O-2H), verapamil (M-CH_2, M-2xCH_2 and M+O-2H), and amodiaquine (M+O) on a TiO_2-coated glass wafer (see Table 1 for examples of the reactions). M-CH_2 product of verapamil ≥ 2 isomers: 1. O-demethylation of B ring and 2. O-demethylation of A-ring or N-demethylation (the alternative reaction sites are italicized). M-2xCH_2 products of verapamil ≥ 2 isomers: 1. O-demethylation of B ring and O-demethylation of A-ring or N-demethylation, 2. O-demethylation of A-ring and N-demethylation or 2x O-demethylation of A-ring.*

5 Conclusions and future perspectives

Developing clever methods to investigate biologically relevant oxidation reactions is essential, as redox reactions play a major role in several physiological and pathophysiological processes such as oxidative stress, which causes oxidative damage to biological macromolecules, and drug metabolism. TiO_2 photocatalysis is an interesting option for imitation of biological oxidation reactions, as it produces several oxidizing species enabling several oxidation mechanisms; hydroxyl radicals, superoxide, and singlet oxygen can be formed in TiO_2 photocatalysis, making it a potential technique to study oxidative modifications of biological macromolecules caused by ROS that are also involved in oxidative stress. In CYP450-catalyzed oxidative drug metabolism, two common initiation mechanisms are hydrogen atom transfer and electron transfer from the substrate molecule to the enzyme. TiO_2 photocatalysis enables both of these mechanisms, as hydroxyl radicals can abstract hydrogen atoms and holes on the TiO_2 surface can accept electrons from the substrate. Direct electrochemical oxidation is limited to reactions beginning with single electron transfer, whereas the hydroxyl radical-based methods, such as EC-Fenton, enable only hydrogen atom abstraction or addition of hydroxyl radicals to unsaturated bonds. Furthermore, TiO_2 photocatalysis is a nonhazardous oxidation method and easily accessible, as TiO_2 particles and UV lamps are commercially available as well as relatively inexpensive. The photocatalytic reaction can be easily controlled by UV exposure time, and no other specific instrumentation is needed.

In this work, TiO_2 photocatalysis proved to be a feasible, fast, and simple method for oxidation of compounds with different polarities. TiO_2 photocatalysis was, for the first time, used to study oxidation reactions of phosphorylated peptides. The hydroxyl radical-initiated oxidation resulted mainly in hydroxylation of nonphosphorylated tyrosine, whereas phosphorylation generally protected the tyrosine residue from oxidation. It should be assessed whether phosphorylation is involved in controlling oxidation of tyrosine residues *in vivo*, in order to open up new research targets. Other interesting applications concerning oxidation of biomolecules could be determination of the location of the double bond in unknown unsaturated lipids and oxidation of oligonucleotides.

TiO_2 photocatalysis imitated 44% and 31% of the phase I HLM metabolites of the model drugs and anabolic steroids, respectively, and performed better in imitation of phase I HLM metabolism than did EC-Fenton or direct EC. This can be explained by the mechanistic differences of the three imitation methods discussed above. All of the compared imitation methods produced too few metabolites and too many nonmetabolic products, and thus, none of them can be used for exact prediction of drug metabolites. The enzymatic reactions are highly selective and their diversity cannot be imitated adequately by a method with different selectivity, such as EC, or by relatively nonselective methods, such as TiO_2 photocatalysis and EC-Fenton. For comparison, computational methods have been shown to correctly predict 50-90% of the most likely sites of metabolism,[168-172] and to rival the biotransformation experts in prediction accuracy.[168-169] Nevertheless, the *in silico* methods that predict metabolites instead of sites of metabolism tend to predict too many false metabolites because of the various combinations of metabolic reactions.[171-172] It seems unlikely that the *in silico* methods would completely abolish the need for *in vitro* and *in vivo*

metabolism experiments in the near future. It is noteworthy, however, that neither the *in vitro* metabolism experiments nor the animal experiments can exactly predict the human *in vivo* metabolism of a drug, yet these experiments provide other essential information, such as pharmacokinetic data, which cannot be derived from the imitation reactions. Even though the correlation of TiO_2 photocatalytic products and the HLM metabolites was far from perfect, TiO_2 photocatalysis may aid in compound optimization by revealing easily oxidizable spots in a drug molecule, which can potentially be metabolically susceptible sites as well.

The imitation methods may provide straightforward approaches for rapid and low-cost synthesis of metabolite standards, obviating the need to develop multistep synthetic strategies or to purify compounds present in complex biological matrices, especially when these are not easily obtained by other methods. Nonetheless, fractionation is needed for purification of specific compounds, as a mixture of large number of compounds is usually obtained, particularly with TiO_2 photocatalysis and EC-Fenton, which enable hydroxylation of various sites. TiO_2 photocatalysis, being much faster than EC-Fenton or the enzymatic *in vitro* metabolism assays, can provide an extremely rapid and inexpensive way to produce aliphatic and aromatic hydroxylation products. Hence, an interesting use of TiO_2 photocatalysis, in addition to rapid synthesis of standards, could be diversification of hit or lead compounds, i.e. production of multiple hydroxylated derivatives of bioactive compounds, which may have improved activity, selectivity, or bioavailability relative to the original molecule. The preparative applications require scaling up, which should, however, be possible considering that TiO_2 photocatalysis has been used for waste water treatment applications, where the volumes are large. EC has been widely used for studying reactive metabolites,[173] and glutathione conjugation of a reactive metabolite of paracetamol produced by TiO_2 photocatalysis has also been demonstrated.[46] Thus, the wider applicability of TiO_2 photocatalysis for studying reactive intermediates could be an interesting area for future research.

Simple integration of TiO_2 photocatalytic reactions into DESI-MS analysis by using the same TiO_2-coated glass wafer as a sample platform for the photocatalysis and DESI-MS analysis omitted the need for the time-consuming removal of TiO_2 particles prior to sample analysis and enhanced the speed of analysis considerably. Thus, the TiO_2 photocatalysis–DESI-MS rotating array platform enabled high-throughput screening of photocatalytic oxidation products as well as imitation of some drug metabolism reactions, even though the isomeric products could not be identified exactly. The major advantages of the TiO_2 photocatalysis–DESI-MS rotating array platform include straightforward fabrication, low sample consumption, and quick experiments to study biologically relevant oxidation reactions. The rotating platform can be further applied to investigate various catalytic reactions and combined with ambient mass spectrometric analysis using techniques other than DESI, e.g. direct analysis in real time, desorption atmospheric pressure photoionization, and various plasma-based techniques. The system could also be applied to photodegradation studies, with or without TiO_2 coating, to support the study of photostability and environmental burden of drugs and other compounds. For instance, an analogous system, integrating an UV lamp above the DESI-MS spot, could enable online monitoring of photostability of solid drug formulations or active pharmaceutical ingredients.

In conclusion, TiO_2 photocatalysis offers a rapid, inexpensive, and simple approach for oxidation of diverse compounds. With appropriate development in the future, the most feasible use of TiO_2 photocatalysis in drug discovery and development is likely to be synthesis of metabolites or other more hydrophilic derivatives of bioactive compounds. However, probably a more interesting use of TiO_2 photocatalysis is studying oxidation of various biomolecules. In addition, TiO_2 photocatalysis may help in identification of environmental transformation products of drugs, pesticides, and other environmental pollutants and in their production for toxicity testing.

References

[1] Butterfield, D.A., Lauderback, C.M., 2002. Lipid peroxidation and protein oxidation in Alzheimer's disease brain: Potential causes and consequences involving amyloid beta-peptide-associated free radical oxidative stress. Free Radical Biol. Med. 32, 1050-1060.

[2] Butterfield, D.A., Perluigi, M., Reed, T., Muharib, T., Hughes, C.P., Robinson, R.A.S., Sultana, R., 2012. Redox proteomics in selected neurodegenerative disorders: from its infancy to future applications. Antiox. Redox Signaling 17, 1610-1655.

[3] Rani, V., Deep, G., Singh, R.K., Palle, K., Yadav, U.C.S., 2016. Oxidative stress and metabolic disorders: Pathogenesis and therapeutic strategies. Life Sci. 148, 183-193.

[4] Adibhatla, R.M., Hatcher, J.F., 2010. Lipid oxidation and peroxidation in CNS health and disease: from molecular mechanisms to therapeutic opportunities. Antiox. Redox Signaling 12, 125-169.

[5] Reuter, S., Gupta, S.C., Chaturvedi, M.M., Aggarwal, B.B., 2010. Oxidative stress, inflammation, and cancer: How are they linked? Free Radical Biol. Med. 49, 1603-1616.

[6] Guengerich, F.P., 2008. Cytochrome P450 and chemical toxicology. Chem. Res. Toxicol. 21, 70-83.

[7] Rendic, S., Guengerich, F.P., 2012. Contributions of human enzymes in carcinogen metabolism. Chem. Res. Toxicol. 25, 1316-1383.

[8] Davies, M.J., 2005. The oxidative environment and protein damage. Biochem. Biophys. Acta 1703, 93-109.

[9] Pisoschi, A.M., Pop, A., 2015. The role of antioxidants in the chemistry of oxidative stress: A review. Eur. J. Med. Chem. 97, 55-74.

[10] Sharma, V.K., Rokita, S.E., 2012. Wiley series of reactive intermediates in chemistry and biology: Oxidation of amino acids, peptides, and proteins: kinetics and mechanism. John Wiley & Sons, Somerset, NJ, USA.

[11] Du, J., Gebicki, J.M., 2004. Proteins are major initial cell targets of hydroxyl free radicals. Int. J. Biochem. Cell Biol. 36, 2334-2343.

[12] Feeney, M.B., Schöneich, C., 2012. Tyrosine modifications in aging. Antiox. Redox Signaling 17, 1571-1579.

[13] Pelkonen, O., Turpeinen, M., Hakkola, J., Honkakoski, P., Hukkanen, J., Raunio, H., 2008. Inhibition and induction of human cytochrome P450 enzymes: current status. Arch. Toxicol. 82, 667-715.

[14] Guengerich, F.P., 2001. Common and uncommon cytochrome P450 reactions related to metabolism and chemical toxicity. Chem. Res. Toxicol. 14, 611-650.

[15] Park, B.K., Boobis, A., Clarke, S., Goldring, C.E.P., Jones, D., Kenna, J.G., Lambert, C., Laverty, H.G., Naisbitt, D.J., Nelson, S., Nicoll-Griffith, D.A., Obach, R.S., Routledge, P., Smith, D.A., Tweedie, D.J., Vermeulen, N., Williams, D.P., Wilson, I.D., Baillie, T.A., 2011. Managing the challenge of chemically reactive metabolites in drug development. Nat. Rev. Drug Discovery 10, 292-306.

[16] Guengerich, F.P., 2013. Kinetic deuterium isotope effects in cytochrome P450 oxidation reactions. J. Labelled Compd. Radiopharm. 56, 428-431.

[17] Pelkonen, O., Turpeinen, M., Uusitalo, J., Rautio, A., Raunio, H., 2005. Prediction of drug metabolism and interactions on the basis of in vitro investigations. Basic Clin. Pharmacol. Toxicol. 96, 167-175.

[18] Gómez-Lechón, M., Donato, M., Castell, J., Jover, R., 2004. Human hepatocytes in primary culture: The choice to investigate drug metabolism in man. Curr. Drug Metab. 5, 443-462.

[19] Lohmann, W., Karst, U., 2008. Biomimetic modeling of oxidative drug metabolism. Anal. Bioanal Chem. 391, 79-96.

[20] Pritchard, J.F., Jurima-Romet, M., Reimer, M.L.J., Mortimer, E., Rolfe, B., Cayen, M.N., 2003. Making better drugs: Decision gates in non-clinical drug development. Nat. Rev. Drug Discovery 2, 542-553.

[21] Roeser, J., Bischoff, R., Bruins, A.P., Permentier, H.P., 2010. Oxidative protein labeling in mass-spectrometry-based proteomics. Anal. Bioanal. Chem. 397, 3441-3455.

[22] Xu, G., Chance, M.R., 2007. Hydroxyl radical-mediated modification of proteins as probes for structural proteomics. Chem. Rev. 107, 3514-3543.

[23] Permentier, H.P., Bruins, A.P., Bischoff, R., 2008. Electrochemistry-mass spectrometry in drug metabolism and protein research. Mini-Rev. Med. Chem. 8, 46-56.

[24] Bernadou, J., Meunier, B., 2004. Biomimetic chemical catalysts in the oxidative activation of drugs. Adv. Synth. Catal. 346, 171-184.

[25] Jurva, U., Wikström, H.V., Weidolf, L., Bruins, A.P., 2003. Comparison between electrochemistry/mass spectrometry and cytochrome P450 catalyzed oxidation reactions. Rapid Commun. Mass Spectrom. 17, 800-810.

[26] Johansson, T., Weidolf, L., Jurva, U., 2007. Mimicry of phase I drug metabolism - novel methods for metabolite characterization and synthesis. Rapid Commun.Mass Spectrom. 21, 2323-2331.

[27] Liang, S., Shiue, Y., Kuo, C., Guo, S., Liao, W., Tsai, E., 2013. Online monitoring oxidative products and metabolites of nicotine by free radicals generation with Fenton reaction in tandem mass spectrometry. Sci. World J. 2013, 189162.

[28] Van der Steen, J., Timmer, E.C., Westra, J.G., Benckhuysen, C., 1973. 4-Hydroperoxidation in Fenton oxidation of antitumor agent cyclophosphamide. J.Am.Chem.Soc. 95, 7535-7536.

[29] Zbaida, S., Kariv, R., Fischer, P., Silman-Greenspan, J., Tashma, Z., 1986. Reaction of cimetidine with Fenton reagent. Eur. J. Biochem. 154, 603-605.

[30] Calza, P., Pazzi, M., Medana, C., Baiocchi, C., Pelizzetti, E., 2004. The photocatalytic process as a tool to identify metabolitic products formed from dopant substances: the case of buspirone. J. Pharm. Biomed. Anal. 35, 9-19.

[31] Nissilä, T., Sainiemi, L., Karikko, M., Kemell, M., Ritala, M., Franssila, S., Kostiainen, R., Ketola, R.A., 2011. Integrated photocatalytic micropillar nanoreactor electrospray ionization chip for mimicking phase I metabolic reactions. Lab Chip 11, 1470-1476.

[32] Kugelmann, E., Albert, C.R., Bringmann, G., Holzgrabe, U., 2011. Fenton's oxidation: A tool for the investigation of potential drug metabolites. J. Pharm. Biomed. Anal. 54, 1047-1058.

[33] Zbaida, S., Kariv, R., Fischer, P., Gilhar, D., 1987. Reactions of theophylline, theobromine and caffeine with Fenton reagent - Simulation of hepatic-metabolism. Xenobiotica 17, 617-621.

[34] Oturan, M.A., Pinson, J., Oturan, N., Deprez, D., 1999. Hydroxylation of aromatic drugs by the electro-Fenton method. Formation and identification of the metabolites of Riluzole. New J. Chem. 23, 793-794.

[35] Oturan, M.A., Pinson, J., Bizot, J., Deprez, D., Terlain, B., 1992. Reaction of inflammation inhibitors with chemically and electrochemically generated hydroxyl radicals. J. Electroanal. Chem. 334, 103-109.

[36] Baumann, A., Lohmann, W., Schubert, B., Oberacher, H., Karst, U., 2009. Metabolic studies of tetrazepam based on electrochemical simulation in comparison to in vivo and in vitro methods. J. Chromatogr. A 1216, 3192-3198.

[37] Gul, T., Bischoff, R., Permentier, H.P., 2017. Mechanism of aromatic hydroxylation of lidocaine at a Pt electrode under acidic conditions. Electrochim. Acta 224, 636-641.

[38] Madsen, K.G., Skonberg, C., Jurva, U., Cornett, C., Hansen, S.H., Johansen, T.N., Olsen, J., 2008. Bioactivation of diclofenac in vitro and in vivo: Correlation to electrochemical studies. Chem. Res. Toxicol. 21, 1107-1119.

[39] Bussy, U., Delaforge, M., El-Bekkali, C., Ferchaud-Roucher, V., Krempf, M., Tea, I., Galland, N., Jacquemin, D., Boujtita, M., 2013. Acebutolol and alprenolol metabolism predictions: comparative study of electrochemical and cytochrome P450-catalyzed reactions using liquid chromatography coupled to high-resolution mass spectrometry. Anal. Bioanal. Chem. 405, 6077-6085.

[40] van Leeuwen, S.M., Blankert, B., Kauffmann, J.M., Karst, U., 2005. Prediction of clozapine metabolism by on-line electrochemistry/liquid chromatography/mass spectrometry. Anal. Bioanal. Chem. 382, 742-750.

[41] Jahn, S., Baumann, A., Roscher, J., Hense, K., Zazzeroni, R., Karst, U., 2011. Investigation of the biotransformation pathway of verapamil using electrochemistry/liquid chromatography/mass spectrometry - A comparative study with liver cell microsomes. J. Chromatogr. A 1218, 9210-9220.

[42] Madsen, K.G., Olsen, J., Skonberg, C., Hansen, S.H., Jurva, U., 2007. Development and evaluation of an electrochemical method for studying reactive phase-I metabolites: Correlation to in vitro drug metabolism. Chem. Res. Toxicol. 20, 821-831.

[43] Lassila, T., Mattila, S., Turpeinen, M., Tolonen, A., 2015. Glutathione trapping of reactive drug metabolites produced by biomimetic metalloporphyrin catalysts. Rapid Commun. Mass Spectrom. 29, 521-532.

[44] Medana, C., Calza, P., Giancotti, V., Dal Bello, F., Pasello, E., Montana, M., Baiocchi, C., 2011. Horse metabolism and the photocatalytic process as a tool to identify metabolic products formed from dopant substances: the case of sildenafil. Drug Test. Anal. 3, 724-734.

[45] Medana, C., Calza, P., Giancotti, V., Dal Bello, F., Aragno, M., Baiocchi, C., 2013. Study of the photocatalytic transformation of synephrine: a biogenic amine relevant in anti-doping analysis. Anal. Bioanal. Chem. 405, 1105-1113.

[46] Raoof, H., Mielczarek, P., Michalow, K.A., Rekas, M., Silberring, J., 2013. Synthesis of metabolites of paracetamol and cocaine via photooxidation on TiO2 catalyzed by UV light. J. Photochem. Photobiol. B 118, 49-57.

[47] Maleknia, S.D., Downard, K.M., 2014. Advances in radical probe mass spectrometry for protein footprinting in chemical biology applications. Chem. Soc. Rev. 43, 3244-3258.

[48] Fenton, H.J.H., 1894. LXXIII.-Oxidation of tartaric acid in presence of iron. J. Chem. Soc., Trans. 65, 899–910.

[49] Haber, V.F., Weiss, J., 1932. Über die Katalyse des Hydroxyperoxydes. Naturwissenschaften 20, 948–950.

[50] Monroe, E.B., Heien, M.L., 2013. Electrochemical generation of hydroxyl radicals for examining protein structure. Anal. Chem. 85, 6185-6189.

[51] Jurva, U., Wikström, H.V., Bruins, A.P., 2002. Electrochemically assisted Fenton reaction: reaction of hydroxyl radicals with xenobiotics followed by on-line analysis with high-performance liquid chromatography/tandem mass spectrometry. Rapid Commun. Mass Spectrom. 16, 1934-1940.

[52] Maleknia, S.D., Brenowitz, M., Chance, M.R., 1999. Millisecond radiolytic modification of peptides by synchrotron X-rays identified by mass spectrometry. Anal. Chem. 71, 3965-3973.

[53] Maleknia, S.D., Kiselar, J.G., Downard, K.M., 2002. Hydroxyl radical probe of the surface of lysozyme by synchrotron radiolysis and mass spectrometry. Rapid Commun. Mass Spectrom. 16, 53-61.

[54] Tong, X., Wren, J.C., Konermann, L., 2008. Gamma-ray-mediated oxidative labeling for detecting protein conformational changes by electrospray mass spectrometry. Anal. Chem. 80, 2222-2231.

[55] Watson, C., Janik, I., Zhuang, T., Charvátová, O., Woods, R.J., Sharp, J.S., 2009. Pulsed electron beam water radiolysis for submicrosecond hydroxyl radical protein footprinting. Anal. Chem. 81, 2496-2505.

[56] Zhang, H., Gau, B.C., Jones, L.M., Vidavsky, I., Gross, M.L., 2011. Fast photochemical oxidation of proteins for comparing structures of protein-ligand complexes: The calmodulin-peptide model system. Anal. Chem. 83, 311-318.

[57] Maleknia, S.D., Chance, M.R., Downard, K.M., 1999. Electrospray-assisted modification of proteins: a radical probe of protein structure. Rapid Commun. Mass Spectrom. 13, 2352-2358.

[58] Xu, G., Chance, M.R., 2005. Radiolytic modification and reactivity of amino acid residues serving as structural probes for protein footprinting. Anal. Chem. 77, 4549-4555.

[59] Liu, F., Lai, S., Tong, H., Lakey, P.S.J., Shiraiwa, M., Weller, M.G., Pöschl, U., Kampf, C.J., 2017. Release of free amino acids upon oxidation of peptides and proteins by hydroxyl radicals. Anal. Bioanal. Chem. 409, 2411-2420.

[60] Shum, W., Maleknia, S.D., Downard, K.M., 2005. Onset of oxidative damage in alpha-crystallin by radical probe mass-spectrometry. Anal. Biochem. 344, 247-256.

[61] Baron, C.P., Refsgaard, H.H.F., Skibsted, L.H., Andersen, M.L., 2006. Oxidation of bovine serum albumin initiated by the Fenton reaction - effect of EDTA, tert-butylhydroperoxide and tetrahydrofuran. Free Radic.Res. 40, 409-417.

[62] Sharp, J.S., Becker, J.M., Hettich, R.L., 2003. Protein surface mapping by chemical oxidation: Structural analysis by mass spectrometry. Anal. Biochem. 313, 216-225.

[63] Wong, J.W.H., Maleknia, S.D., Downard, K.M., 2005. Hydroxyl radical probe of the calmodulin-melittin complex interface by electrospray ionization mass spectrometry. J. Am. Soc. Mass Spectrom. 16, 225-233.

[64] Leser, M., Pegan, J., El Makkaoui, M., Schlatterer, J.C., Khine, M., Law, M., Brenowitz, M., 2015. Protein footprinting by pyrite shrink-wrap laminate. Lab Chip 15, 1646-1650.

[65] Bisby, R.H., Tabassum, N., 1988. Properties of the radicals formed by one-electron oxidation of acetaminophen—A pulse radiolysis study. Biochem. Pharmacol. 37, 2731-2738.

[66] Bisby, R.H., 1990. Reactions of a free radical intermediate in the oxidation of amodiaquine. Biochem. Pharmacol. 39, 2051-2055.

[67] Ismail, F.M.D., Drew, M.G.B., Navaratnam, S., Bisby, R.H., 2009. A pulse radiolysis study of free radicals formed by one-electron oxidation of the antimalarial drug pyronaridine. Res. Chem. Intermed. 35, 363-377.

[68] Bussy, U., Boujtita, M., 2014. Advances in the electrochemical simulation of oxidation reactions mediated by cytochrome P450. Chem. Res. Toxicol. 27, 1652-1668.

[69] Permentier, H.P., Jurva, U., Barroso, B., Bruins, A.P., 2003. Electrochemical oxidation and cleavage of peptides analyzed with on-line mass spectrometric detection. Rapid Commun. Mass Spectrom. 17, 1585-1592.

[70] Permentier, H.P., Bruins, A.P., 2004. Electrochemical oxidation and cleavage of proteins with on-line mass spectrometric detection: development of an instrumental alternative to enzymatic protein digestion. J. Am. Soc. Mass Spectrom. 15, 1707-1716.

[71] Maleknia, S.D., Johnson, R., 2012. Mass Spectrometry of Amino Acids and Proteins. In: Hughes, A. (Ed.), Amino acids, peptides and proteinds in organic chemistry, Vol. 5: Analysis and function of amino acids and peptides. Wiley-VCH Verlag GmbH, Weinheim, Germany, pp. 1-50.

[72] Kerman, K., Vestergaard, M., Chikae, M., Yamamura, S., Tamiya, E., 2007. Label-free electrochemical detection of the phosphorylated and non-phosphorylated forms of peptides based on tyrosine oxidation. Electrochem. Commun. 9, 976-980.

[73] Qu, N., Wan, B., Guo, L., 2008. Label-free electrochemical differentiation of phosphorylated and non-phosphorylated peptide by electro-catalyzed tyrosine oxidation. Analyst 133, 1246-1249.

[74] Hunter, T., 2000. Signaling - 2000 and beyond. Cell 100, 113-127.

[75] Nouri-Nigjeh, E., Bischoff, R., Bruins, A.P., Permentier, H.P., 2011. Electrochemistry in the mimicry of oxidative drug metabolism by cytochrome P450s. Curr. Drug Metab. 12, 359-371.

[76] Lohmann, W., Karst, U., 2009. Electrochemistry meets enzymes: instrumental on-line simulation of oxidative and conjugative metabolism reactions of toremifene. Anal. Bioanal. Chem. 394, 1341-1348.

[77] Jirásko, R., Mikysek, T., Chagovets, V., Vokřál, I., Holčapek, M., 2013. Structural characterization of electrochemically and in vitro biologically generated oxidation products of atorvastatin using UHPLC/MS/MS. Anal. Bioanal. Chem. 405, 7181-7193.

[78] Sono, M., Roach, M.P., Coulter, E.D., Dawson, J.H., 1996. Heme-containing oxygenases. Chem. Rev. 96, 2841-2888.

[79] CarvalhoDa-Silva, D., Mac Leod, T.C.O., de Faria, A.L., dos Santos, J.S., Dai de Carvalho, M. E. M., Rebouças, J.S., Idemori, Y.M., das Dores Assis, M., 2011. Carbamazepine oxidation catalyzed by manganese porphyrins: Effects of the β-bromination of the macrocycle and the choice of oxidant. Appl. Catal., A 408, 25-30.

[80] Chauhan, S.M.S., Kandadai, S.A., Kumar, A., 2002. Biomimetic reduction of nimesulide with $NaBH_4$ catalyzed by metalloporphyrins. Chem. Pharm. Bull. 50, 1421-1422.

[81] Balogh, G.T., Keseru, G.M., 2004. Metalloporphyrin mediated biomimetic oxidations. A useful tool for the investigation of cytochrome P450 catalyzed oxidative metabolism. Arkivoc, 124-139.

[82] Othman, S., Mansuy-Mouries, V., Bensoussan, C., Battioni, P., Mansuy, D., 2000. Hydroxylation of diclofenac: an illustration of the complementary roles of biomimetic metalloporphyrin catalysts and yeasts expressing human cytochromes P450 in drug metabolism studies. C. R. Acad. Sci., Ser. IIc: Chim. 3, 751-755.

[83] Bochot, C., Bartoli, J., Frapart, Y., Dansette, P.M., Mansuy, D., Battioni, P., 2007. Synthesis and spectroscopic, electrochemical, and catalytic properties of a new manganese porphyrin bearing four positive charges close to the metal. J. Mol. Catal. A: Chem. 263, 200-205.

[84] Chauhan, S.M.S., Kandadai, S.A., Sahoo, B., 2001. Regioselective biomimetic oxidation of etodolac with iodosylbenzene catalyzed by halogenated and perhalogenated metalloporphyrins in dichloromethane. Chem. Pharm. Bull. 49, 1375-1376.

[85] Mac Leod, T.C.O., Faria, A.L., Barros, V.P., Queiroz, M.E.C., Assis, M.D., 2008. Primidone oxidation catalyzed by metalloporphyrins and Jacobsen catalyst. J. Mol. Catal. A: Chem. 296, 54-60.

[86] Melo, A.J.B., Iamamoto, Y., Maestrin, A.P.J., Lindsay Smith, J.R., Santos, M.D., Lopes, N.P., Bonato, P.S., 2005. Biomimetic oxidation of praziquantel catalysed by metalloporphynins. J. Mol. Catal. A: Chem. 226, 23-31.

[87] Neves, C.M.B., Simoes, M.M.Q., Domingues, M.R.M., Santos, I.C.M.S., Neves, M.G.P.M.S., Almeida Paz, F.A., Silva, A.M.S., Cavaleiro, J.A.S., 2012. Oxidation of diclofenac catalyzed by manganese porphyrins: synthesis of novel diclofenac derivatives. Rsc Advances 2, 7427-7438.

[88] Breslow, R., Huang, Y., Zhang, X., Yang, J., 1997. An artificial cytochrome P450 that hydroxylates unactivated carbons with regio- and stereoselectivity and useful catalytic turnovers. Proc. Natl. Acad. Sci. U. S. A. 94, 11156-11158.

[89] Fang, Z., Breslow, R., 2006. Metal coordination-directed hydroxylation of steroids with a novel artificial P-450 catalyst. Org. Lett. 8, 251-254.

[90] Stuk, T.L., Grieco, P.A., Marsh, M.M., 1991. Site-selective hydroxylation of steroids via oxometalloporphinates covalently linked to ring-D: Introduction of hydroxyl-groups into the C(9) and C(12) position of 5α-androstanes. J. Org. Chem. 56, 2957-2959.

[91] Yang, J., Breslow, R., 2000. Selective hydroxylation of a steroid at C-9 by an artificial cytochrome P-450. Angew. Chem. Int. Ed. Engl. 39, 2692-2694.

[92] Akagah, B., Lormier, A.T., Fournet, A., Figadere, B., 2008. Oxidation of antiparasitic 2-substituted quinolines using metalloporphyrin catalysts: scale-up of a biomimetic reaction for metabolite production of drug candidates. Org. Biomol. Chem. 6, 4494-4497.

[93] HepatoChem Inc., http://www.hepatochem.com/ 2017.

[94] Fujishima, A., Rao, T.N., Tryk, D.A., 2000. Titanium dioxide photocatalysis. J. Photochem. Photobiol. C: Photochem. Rev. 1, 1-21.

[95] Luttrell, T., Halpegamage, S., Tao, J., Kramer, A., Sutter, E., Batzill, M., 2014. Why is anatase a better photocatalyst than rutile? - Model studies on epitaxial TiO_2 films. Sci. Rep. 4, 4043.

[96] Xu, M., Gao, Y., Moreno, E.M., Kunst, M., Muhler, M., Wang, Y., Idriss, H., Wöll, C., 2011. Photocatalytic activity of bulk TiO_2 anatase and rutile single crystals using infrared absorption spectroscopy. Phys. Rev. Lett. 106, 138302.

[97] Zhang, J., Zhou, P., Liu, J., Yu, J., 2014. New understanding of the difference of photocatalytic activity among anatase, rutile and brookite TiO_2. Phys. Chem. Chem. Phys. 16, 20382-20386.

[98] Hurum, D.C., Agrios, A.G., Gray, K.A., Rajh, T., Thurnauer, M.C., 2003. Explaining the enhanced photocatalytic activity of Degussa P25 mixed-phase TiO_2 using EPR. J. Phys. Chem. B 107, 4545-4549.

[99] Fujishima, A., Zhang, X., Tryk, D.A., 2008. TiO_2 photocatalysis and related surface phenomena. Surf. Sci. Rep. 63, 515-582.

[100] Nosaka, Y., Daimon, T., Nosaka, A.Y., Murakami, Y., 2004. Singlet oxygen formation in photocatalytic TiO_2 aqueous suspension. Phys. Chem. Chem. Phys. 6, 2917-2918.

[101] Daimon, T., Hirakawa, T., Kitazawa, M., Suetake, J., Nosaka, Y., 2008. Formation of singlet molecular oxygen associated with the formation of superoxide radicals in aqueous suspensions of TiO_2 photocatalysts. Appl. Catal., A 340, 169-175.

[102] Daimon, T., Nosaka, Y., 2007. Formation and behavior of singlet molecular oxygen in TiO_2 photocatalysis studied by detection of near-infrared phosphorescence. J. Phys. Chem. C 111, 4420-4424.

[103] Daimon, T., Hirakawa, T., Nosaka, Y., 2008. Monitoring the formation and decay of singlet molecular oxygen in TiO_2 photocatalytic systems and the reaction with organic molecules. Electrochemistry 76, 136-139.

[104] Bhatkhande, D.S., Pangarkar, V.G., Beenackers, A.A.C.M., 2002. Photocatalytic degradation for environmental applications - a review. J. Chem. Tech. Biotech. 77, 102-116.

[105] Pelton, R., Geng, X., Brook, M., 2006. Photocatalytic paper from colloidal TiO_2—fact or fantasy. Adv. Colloid Interface Sci. 127, 43-53.

[106] Larsen, M.R., Thingholm, T.E., Jensen, O.N., Roepstorff, P., Jørgensen, T.J.D., 2005. Highly selective enrichment of phosphorylated peptides from peptide mixtures using titanium dioxide microcolumns. Mol. Cell. Proteomics 4, 873-886.

[107] Liang, S., Makamba, H., Huang, S., Chen, S., 2006. Nano-titanium dioxide composites for the enrichment of phosphopeptides. J. Chromatogr. A 1116, 38-45.

[108] Thingholm, T.E., Jørgensen, T.J.D., Jensen, O.N., Larsen, M.R., 2006. Highly selective enrichment of phosphorylated peptides using titanium dioxide. Nat. Protoc. 1, 1929-1935.

[109] Elsellami, L., Vocanson, F., Dappozze, F., Puzenat, E., Païsse, O., Houas, A., Guillard, C., 2010. Kinetic of adsorption and of photocatalytic degradation of phenylalanine effect of pH and light intensity. Appl. Catal., A 380, 142-148.

[110] Yang, H., An, T., Li, G., Song, W., Cooper, W.J., Luo, H., Guo, X., 2010. Photocatalytic degradation kinetics and mechanism of environmental pharmaceuticals in aqueous suspension of TiO_2: A case of β-blockers. J. Hazard. Mater. 179, 834-839.

[111] Carrier, M., Perol, N., Herrmann, J., Bordes, C., Horikoshi, S., Paisse, J.O., Baudot, R., Guillard, C., 2006. Kinetics and reactional pathway of Imazapyr photocatalytic degradation Influence of pH and metallic ions. Appl. Catal., B 65, 11-20.

[112] Sakkas, V.A., Calza, P., Medana, C., Villioti, A.E., Baiocchi, C., Pelizzetti, E., Albanis, T., 2007. Heterogeneous photocatalytic degradation of the pharmaceutical agent salbutamol in aqueous titanium dioxide suspensions. Appl. Catal., B 77, 135-144.

[113] Jones, B.J., Vergne, M.J., Bunk, D.M., Locascio, L.E., Hayes, M.A., 2007. Cleavage of peptides and proteins using light-generated radicals from titanium dioxide. Anal. Chem. 79, 1327-1332.

[114] Antoniou, M.G., Shoemaker, J.A., De la Cruz, A.A., Dionysiou, D.D., 2008. Unveiling new degradation intermediates/pathways from the photocatalytic degradation of microcystin-LR. Environ. Sci. Technol. 42, 8877-8883.

[115] Liu, I., Lawton, L.A., Robertson, P.K.J., 2003. Mechanistic studies of the photocatalytic oxidation of microcystin-LR: an investigation of byproducts of the decomposition process. Environ. Sci. Technol. 37, 3214-3219.

[116] Kostiainen, R., Kotiaho, T., Kuuranne, T., Auriola, S., 2003. Liquid chromatography/atmospheric pressure ionization-mass spectrometry in drug metabolism studies. J. Mass Spectrom. 38, 357-372.

[117] Prasad, B., Garg, A., Takwani, H., Singh, S., 2011. Metabolite identification by liquid chromatography-mass spectrometry. TrAC, Trends Anal. Chem. 30, 360-387.

[118] Chen, G., Pramanik, B.N., 2009. Application of LC/MS to proteomics studies: current status and future prospects. Drug Discov. Today 14, 465-471.

[119] Han, X., Aslanian, A., Yates, J.R.III, 2008. Mass spectrometry for proteomics. Curr. Opin. Chem. Biol. 12, 483-490.

[120] Zhu, M., Zhang, H., Humphreys, W.G., 2011. Drug metabolite profiling and identification by high-resolution mass spectrometry. J. Biol. Chem. 286, 25419-25425.

[121] Marshall, A.G., Hendrickson, C.L., 2008. High-resolution mass spectrometers. Annu. Rev. Anal. Chem. 1, 579-599.

[122] Maurer, H.H., Meyer, M.R., 2016. High-resolution mass spectrometry in toxicology: current status and future perspectives. Arch. Toxicol. 90, 2161-2172.

[123] Rathahao-Paris, E., Alves, S., Junot, C., Tabet, J., 2016. High resolution mass spectrometry for structural identification of metabolites in metabolomics. Metabolomics 12, 10.

[124] Takamoto, K., Chance, M.R., 2006. Radiolytic protein footprinting with mass Spectrometry to probe the structure of macromolecular complexes. Annu. Rev. Biophys. Biomol. Struct. 35, 251-276.

[125] Takáts, Z., Cotte-Rodriguez, I., Talaty, N., Chen, H., Cooks, R.G., 2005. Direct, trace level detection of explosives on ambient surfaces by desorption electrospray ionization mass spectrometry. Chem. Commun., 1950-1952.

[126] Cody, R.B., Laramee, J.A., Durst, H.D., 2005. Versatile new ion source for the analysis of materials in open air under ambient conditions. Anal. Chem. 77, 2297-2302.

[127] Takáts, Z., Wiseman, J.M., Gologan, B., Cooks, R.G., 2004. Mass spectrometry sampling under ambient conditions with desorption electrospray ionization. Science 306, 471-473.

[128] Haapala, M., Pol, J., Saarela, V., Arvola, V., Kotiaho, T., Ketola, R.A., Franssila, S., Kauppila, T.J., Kostiainen, R., 2007. Desorption atmospheric pressure photoionization. Anal. Chem. 79, 7867-7872.

[129] Costa, A.B., Cooks, R.G., 2007. Simulation of atmospheric transport and droplet-thin film collisions in desorption electrospray ionization. Chem. Commun., 3915-3917.

[130] Venter, A., Sojka, P.E., Cooks, R.G., 2006. Droplet dynamics and ionization mechanisms in desorption electrospray ionization mass spectrometry. Anal. Chem. 78, 8549-8555.

[131] Takáts, Z., Wiseman, J., Cooks, R.G., 2005. Ambient mass spectrometry using desorption electrospray ionization (DESI): instrumentation, mechanisms and applications in forensics, chemistry, and biology. J. Mass Spectrom. 40, 1261-1275.

[132] Iribarne, J.V., Thomson, B.A., 1976. On the evaporation of small ions from charged droplets. J. Chem. Phys. 64, 2284-2294.

[133] Thomson, B.A., Iribarne, J.V., 1979. Field induced ion evaporation from liquid surfaces at atmospheric pressure. J. Chem. Phys. 71, 4451-4463.

[134] Dole, M., Mack, L.L., Hines, R.L., Mobley, R.C., Ferguson, L.D., Alice, M.B., 1968. Molecular beams of macroions. J. Chem. Phys. 49, 2240-2249.

[135] Li, X., 2013. Solvent effects and improvements in the deoxyribose degradation assay for hydroxyl radical-scavenging. Food Chem. 141, 2083-2088.

[136] Wójcikowski, J., Pichard-Garcia, L., Maurel, P., Daniel, W.A., 2003. Contribution of human cytochrome p-450 isoforms to the metabolism of the simplest phenothiazine neuroleptic promazine. Br. J. Pharmacol. 138, 1465-74.

[137] Krauser, J.A., Voehler, M., Tseng, L., Schefer, A.B., Godejohann, M., Guengerich, F.P., 2004. Testosterone 1β-hydroxylation by human cytochrome P450 3A4. Eur. J. Biochem. 271, 3962-3969.

[138] Choi, M.H., Skipper, P.L., Wishnok, J.S., Tannenbaum, S.R., 2005. Characterization of testosterone 11β-hydroxylation catalyzed by human liver microsomal cytochromes P450. Drug Metab. Dispos. 33, 714-718.

[139] Zhu, M., Zhao, W., Jimenez, H., Zhang, D., Yeola, S., Dai, R., Vachharajani, N., Mitroka, J., 2005. Cytochrome P450 3A-mediated metabolism of buspirone in human liver microsomes. Drug Metab. Dispos. 33, 500-507.

[140] Zhang, H., Grubb, M., Wu, W., Josephs, J., Humphreys, W.G., 2009. Algorithm for thorough background subtraction of high-resolution LC/MS data: application to obtain clean product ion spectra from nonselective collision-induced dissociation experiments. Anal. Chem. 81, 2695-2700.

[141] Li, A.C., Ding, J., Jiang, X., Denissen, J., 2009. Two-injection workflow for a liquid chromatography/LTQ-Orbitrap system to complete in vivo biotransformation characterization: demonstration with buspirone metabolite identification. Rapid Commun. Mass Spectrom. 23, 3003-3012.

[142] Blankert, B., Hayen, H., van Leeuwen, S.M., Karst, U., Bodoki, E., Lotrean, S., Sandulescu, R., Diez, N.M., Dominguez, O., Arcos, J., Kauffmann, J.M., 2005.

Electrochemical, chemical and enzymatic oxidations of phenothiazines. Electroanalysis 17, 1501-1510.

[143] Bullock, P., Pearce, R., Draper, A., Podval, J., Bracken, W., Veltman, J., Thomas, P., Parkinson, A., 1995. Induction of liver microsomal cytochrome-P450 in cynomolgus monkeys. Drug Metab. Dispos. 23, 736-748.

[144] Yamazaki, H., Shimada, T., 1997. Progesterone and testosterone hydroxylation by cytochromes P450 2C19, 2C9, and 3A4 in human liver microsomes. Arch. Biochem. Biophys. 346, 161-169.

[145] Jung, B., Graf, H., Ullrich, V., 1985. A new monooxygenase product from 7-ethoxycoumarin and its relation to the O-dealkylation reaction. Biol. Chem. Hoppe-Seyler 366, 23-31.

[146] Fisher, M.B., Jackson, D., Kaerner, A., Wrighton, S.A, Borel, A.G., 2002. Characterization by liquid chromatography-nuclear magnetic resonance spectroscopy and liquid chromatography-mass spectrometry of two coupled oxidative-conjugative metabolic pathways for 7-ethoxycoumarinin human liver microsomes treated with alamethicin. Drug Metab. Dispos. 30, 270-275.

[147] Schänzer, W., 1996. Metabolism of anabolic androgenic steroids. Clin. Chem. 42, 1001-1020.

[148] Pozo, Ó.J., Van Eenoo, P., Deventer, K., Lootens, L., Van Thuyne, W., Parr, M.K., Schänzer, W., Sancho, J.V., Hernandez, F., Meuleman, P., Leroux-Roels, G., Delbeke, F.T., 2009. Detection and characterization of a new metabolite of 17 alpha-methyltestosterone. Drug Metab. Dispos. 37, 2153-2162.

[149] Massé, R., Ayotte, C., Bi, H., Dugal, R., 1989. Studies on anabolic-steroids III. Detection and characterization of stanozolol urinary metabolites in humans by gas-chromatography mass-spectrometry. J. Chromatogr. B. Biomed. Appl. 497, 17-37.

[150] Pozo, O.J., Van Eenoo, P., Deventer, K., Lootens, L., Grimalt, S., Sancho, J.V., Hernández, F., Meuleman, P., Leroux-Roels, G., Delbeke, F.T., 2009. Detection and structural investigation of metabolites of stanozolol in human urine by liquid chromatography tandem mass spectrometry. Steroids 74, 837-852.

[151] Poelmans, S., De Wasch, K., De Brabander, H.F., Van de Wiele, M., Courtheyn, D., van Ginkel, L.A., Sterk, S.S., Delahaut, P., Dubois, M., Schilt, R., Nielen, M., Vercammen, J., Impens, S., Stephany, R., Hamoir, T., Pottie, G., Van Poucke, C., Van Peteghem, C., 2002. Analytical possibilities for the detection of stanozolol and its metabolites. Anal. Chim. Acta 473, 39-47.

[152] Biddle, S.T.B., O'Donnell, A., Houghton, E., Creaser, C., 2009. Metabolism of methyltestosterone in the greyhound. Rapid Commun. Mass Spectrom. 23, 713-721.

[153] Blokland, M.H., van Rossum, H.J., Herbold, H.A., Sterk, S.S., Stephany, R.W., van Ginkel, L.A., 2005. Metabolism of methyltestosterone, norethandrolone and methylboldenone in a heifer. Anal. Chim. Acta 529, 317-323.

[154] Roig, M., Segura, J., Ventura, R., 2007. Quantitation of 17 beta-nandrolone metabolites in boar and horse urine by gas chromatography-mass spectrometry. Anal. Chim. Acta 586, 184-195.

[155] Scarth, J.P., Spencer, H.A., Hudson, S.C., Teale, P., Gray, B.P., Hillyer, L.L., 2010. The application of in vitro technologies to study the metabolism of the androgenic/anabolic steroid stanozolol in the equine. Steroids 75, 57-69.

[156] Parr, M.K., Zöllner, A., Fußhöller, G., Opfermann, G., Schlörer, N., Zorio, M., Bureik, M., Schänzer, W., 2012. Unexpected contribution of cytochrome P450 enzymes CYP11B2 and CYP21, as well as CYP3A4 in xenobiotic androgen elimination – Insights from metandienone metabolism. Toxicol. Lett. 213, 381-391.

[157] Schänzer, W., Geyer, H., Donike, M., 1991. Metabolism of metandienone in man - Identification and synthesis of conjugated excreted urinary metabolites, determination of excretion rates and gas-chromatographic mass-spectrometric identification of bis-hydroxylated metabolites. J. Steroid Biochem. Mol. Biol. 38, 441-464.

[158] Wu, S., Zhang, K., Kaiser, N.K., Bruce, J.E.; Prior, D.C.; Anderson G.A., 2006. Incorporation of a flared inlet capillary tube on a Fourier transform ion cyclotron resonance mass spectrometer. J. Am. Soc. Mass Spectrom. 17, 772-779.

[159] Da Costa, C., Reynolds, J.C., Whitmarsh, S., Lynch, T., Creaser, C.S., 2013. The quantitative surface analysis of an antioxidant additive in a lubricant oil matrix by desorption electrospray ionization mass spectrometry. Rapid Commun. Mass Spectrom. 27, 2420-2424.

[160] Gurdak, E., Green, F.M., Rakowska, P.D., Seah, M.P., Salter, T.L., Gilmore, I.S., 2014. VAMAS interlaboratory study for desorption electrospray ionization mass spectrometry (DESI MS) intensity repeatability and constancy. Anal. Chem. 86, 9603-9611.

[161] Green, F.M., Stokes, P., Hopley, C., Seah, M.P., Gilmore, I.S., O'Connor, G., 2009. Developing repeatable measurements for reliable analysis of molecules at surfaces using desorption electrospray ionization. Anal. Chem. 81, 2286-2293.

[162] Churchill, F.C., Patchen, L.C, Campbell, C.C., Schwartz, I.K., Nguyen-Dinh, P., Dickinson, C.M., 1985. Amodiaquine as a prodrug - importance of metabolite(s) in the antimalarial effect of amodiaquine in humans. Life Sci. 36, 53-62.

[163] Churchill, F.C.; Mount, D.L.; Patchen, L.C.; Björkman, A., 1986. Isolation, Characterization and Standardization of a Major Metabolite of Amodiaquine by Chromatographic and Spectroscopic Methods. J. Chromatogr. B. Biomed. Appl. 377, 307-318.

[164] Johansson, T.; Jurva, U.; Grönberg, G.; Weidolf, L.; Masimirembwa, C., 2009. Novel Metabolites of Amodiaquine Formed by CYP1A1 and CYP1B1: Structure Elucidation Using Electrochemistry, Mass Spectrometry, and NMR. Drug Metab. Dispos. 37, 571-579.

[165] Li, X.; Björkman, A.; Andersson, T.B., Ridderström, M.; Masimirembwa, C., 2002. Amodiaquine clearance and its metabolism to N-desethylamodiaquine is mediated by CYP2C8: A new high affinity and turnover enzyme-specific probe substrate. J. Pharmacol. Exp. Ther. 300, 399–407.

[166] Zhang, Y.; Vermeulen, N. P. E.; Commandeur, J. N. M., 2017. Characterization of human cytochrome P450 mediated bioactivation of amodiaquine and its major metabolite N-desethylamodiaquine. Br. J. Clin. Pharmacol. 83, 572-583.

[167] Rousu, T., Herttuainen, J., Tolonen, A., 2010. Comparison of triple quadrupole, hybrid linear ion trap triple quadrupole, time-of-flight and LTQ-Orbitrap mass spectrometers in drug discovery phase metabolite screening and identification in vitro - amitriptyline and verapamil as model compounds. Rapid. Commun. Mass Spectrom. 24, 939-957.

[168] Campagna-Slater, V.; Pottel, J.; Therrien, E.; Cantin, L.; Moitessier, N., 2012. Development of a computational tool to rival experts in the prediction of sites of metabolism of xenobiotics by P450s. J. Chem Inf. Model. 52, 2471-2483.

[169] Afzelius, L.; Hasselgren Arnby, C. ;Broo, A.; Carlsson, L.; Isaksson, C.; Jurva, U.; Kjellander, B.; Kolmodin, K.; Nilsson, K.; Raubacher, F.; Weidolf, L., 2007. State-of-the-art tools for computational site of metabolism predictions: Comparative analysis, mechanistical insights, and future applications. Drug Metab. Rev. 39, 61-86.

[170] Ford, K.A.; Ryslik, G.; Sodhi, J.; Halladay, J.; Diaz, D.; Dambach, D.; Masuda, M. 2015. Computational predictions of the site of metabolism of cytochrome P450 2D6 substrates: comparative analysis, molecular docking, bioactivation and toxicological implications. Drug Metab. Rev. 47, 291-319.

[171] T'jollyn, H.; Boussery, K.; Mortishire-Smith, R.J.; Coe, K.; De Boeck, B.; Van Bocxlaer, J.F.; Mannens, G., 2011. Evaluation of three state-of-the-art metabolite prediction software packages (Meteor, MetaSite, and StarDrop) through independent and synergistic use. Drug Metab. Disposition, 39, 2066-2075

[172] Meng, J.; Li, S.; Liu, X.; Zheng, M.; Li, H., 2017. RD-Metabolizer: an integrated and reaction types extensive approach to predict metabolic sites and metabolites of drug-like molecules. Chem. Cent. J., 11, 65

[173] Bussy, U., Boisseau, R., Thobie-Gautier, C., Boujtita, M., 2015. Electrochemistry-mass spectrometry to study reactive drug metabolites and CYP450 simulations. TrAC, Trends Anal. Chem. 70, 67-73.